DESIGN AND DEVELOPMENT OF A MULTIMODAL SELF ADJUSTING VIBRATION ENERGY HARVESTER SYSTEM

LIM CHIN SEONG

FACULTY OF ENGINEERING
UNIVERSITY OF MALAYA
KUALA LUMPUR

2021

DESIGN AND DEVELOPMENT OF A MULTIMODAL SELF ADJUSTING VIBRATION ENERGY HARVESTER SYSTEM

LIM CHIN SEONG

THESIS SUBMITTED IN FULFILMENT OF THE REQUIREMENTS FOR THE MASTERS OF MECHANICAL ENGINEERING

FACULTY OF ENGINEERING
UNIVERSITY OF MALAYA
KUALA LUMPUR

2021

UNIVERSITY OF MALAYA

ORIGINAL LITERARY WORK DECLARATION

Name of Candidate: Lim Chin Seong

[redacted]

Matric No: 17066278

Name of Degree: Master of Mechanical Engineering

Title of Project Dissertation ("this Work"): Design and Development of a Multimodal Self Adjusting Vibration Energy Harvesting System

Field of Study: Vibration Energy Harvesting

I do solemnly and sincerely declare that:

(1) I am the sole author/writer of this Work;
(2) This Work is original;
(3) Any use of any work in which copyright exists was done by way of fair dealing and for permitted purposes and any excerpt or extract from, or reference to or reproduction of any copyright work has been disclosed expressly and sufficiently and the title of the Work and its authorship have been acknowledged in this Work;
(4) I do not have any actual knowledge nor do I ought reasonably to know that the making of this work constitutes an infringement of any copyright work;
(5) I hereby assign all and every rights in the copyright to this Work to the University of Malaya ("UM"), who henceforth shall be owner of the copyright in this Work and that any reproduction or use in any form or by any means whatsoever is prohibited without the written consent of UM having been first had and obtained;
(6) I am fully aware that if in the course of making this Work I have infringed any copyright whether intentionally or otherwise, I may be subject to legal action or any other action as may be determined by UM.

Candidate's Signature [redacted] Date: 26-MAY-2021

Subscribed and solemnly declared before,

Witness's Signature Date: 31 MAY 2021

Name: [redacted]

Designation:

DESIGN & DEVELOPMENT OF A MULTIMODAL SELF ADJUSTING VIBRATION ENERGY HARVESTER SYSTEM

ABSTRACT

Vibration Energy Harvesting Devices have the potential to replace batteries in powering remote sensors. However, the bandwidth of such devices is typically very narrow, and thus, only able to generate sufficient power when the excitation frequency is at the natural frequency of the device. This research aims to design, build and test the behavior of a cantilever beam that has the capability to self-tune its natural frequency mechanically. The self-tuning mechanism is designed based on the observation that vibration causes freely supported disc to rotate, and the mass distribution of an asymmetrical disc changes with the rotary position of the disc, which in turn changes the natural frequency of the cantilever beam. The self-tuning mechanism is found to increase the bandwidth of the testing apparatus as compared to the bandwidth without self-tuning. An improvement of up to 318% was observed between the measured vibration magnitudes of the self-tuning system vs the system without self-tuning. The vibration magnitude is characterized by RMS Acceleration and Displacement as measured by accelerometers and laser displacement sensor. It is expected that higher Acceleration and Displacement would cause more electrical power to be generated when the self-tuning mechanism is combined with energy conversion devices such as piezo-electric elements.

Keywords: Vibration Energy Harvester, Self-Tuning, Wide Bandwidth

REKABENTUK DAN PEMBANGUNAN PENGEKSTRAK TENAGA GETARAN PENGUBAH SENDIRI

ABSTRAK

Peranti pengekstrak tenaga getaran mempunyai potensi untuk menggantikan bateri yang digunakan untuk menguasakan sistem sensor tanpa wayar. Tetapi julat frekuensi peranti seperti ini biasanya amat rendah. Ia hanya boleh menghasilkan tenaga yang mencukupi bila getaran luaran menpunyai frekuensi yang sama dengan frekuensi semula jadi peranti tersebut. Tujuan penyelidikan ini dijalankan adalah untuk mereka, membina dan menguji sesebuah peranti pengekstrak tenaga getaran yang boleh mengubah frekuensi semula jadinya dengan sendiri secara mekanikal. Mekanisma pengubah sendiri direka berdasarkan permerhatian terhadap fenomena dimana getaran boleh menyebabkan cakera yang longgar berputar dengan sendiri dan penyebaran jisim cakera asimetri bergantung kepada posisi putaran cakera tersebut. Ini boleh mengubah frekuensi semula jadi system tersebut. Setelah diuji, mekanisma pengubah sendiri didapati mampu meningkatkan julat frekuensi peranti tersebut berbanding dengan sistem tanpa pengubah frekuensi sendiri. Peningkatan amplitud sebanyak 318% didapati daripada sistem pengubah sendiri berbanding dengan sistem tanpa mekanisma pengubah sendiri. Magnitud getaran dicirikan dengan pecutan dan sesaran R.M.S yang diukur dengan sensor pecutan dan sensor laser. Pecutan dan sesaran yang lebih tinggi dijangka akan menghasilkan kuasa elektrik yang lebih tinggi bila mekanisma pengubah sendiri digunakan bersama dengan peranti pengubah tenaga seperti elemen piezo-electrik.

Keywords: Pengekstrak Tenaga Getaran, Pengubah Sendiri, Julat Frekuensi

ACKNOWLEDGEMENTS

I would also like to take this opportunity and give my sincerest appreciation to my supervisor, Dr. Alex Ong Zhi Chao for his support, expert guidance and assistance throughout this Research Project. This project would not be a success without his guidance and support.

TABLE OF CONTENTS

ABSTRACT 3

Abstrak 4

Acknowledgements 5

Table of Contents 6

List of Figures 9

List of Tables 12

List of Symbols and Abbreviations 13

List of Appendices 14

CHAPTER 1: INTRODUCTION 15

1.1 Background of the project 15

1.2 Problem Statement 16

1.3 Objectives 17

1.4 Scope of the work 17

CHAPTER 2: LITERATURE REVIEW 18

2.1 Energy harvesting systems and their applications 18

2.2 Limitations of batteries 19

2.3 Vibration energy harvesting system 22

2.4 Narrow Frequency Band 26

2.5 Multimodality 27

2.5.1 Multiple Stacked Systems 27

2.5.2 Self-Tuning Systems 29

2.6 Literature Review Summary 32

CHAPTER 3: METHODOLOGY **34**

3.1 Introduction 34

3.2 Execution flow........ 34

3.3 Self-Tuning Vibration Harvester Design 37

3.4 Fabrication........ 41

3.4.1 Cantilever Beam 41

3.4.2 Spacer........ 42

3.4.3 Asymmetrical Disc........ 44

3.4.4 Bolt-Nut-Washer........ 46

3.4.5 Assembly 46

3.5 Experiments to Determine Tuning Behavior 49

3.5.1 Determination of the Natural Frequency of the System 49

3.5.2 Self-Tuning Behavior of the System........ 51

3.5.3 Bandwidth of the System 51

3.5.4 Real Time Amplitude – Self-Tuning 52

CHAPTER 4: RESULTS AND DISCUSSION **54**

4.1 Introduction. 54

4.2 Self-Tuning Vibration Harvester Design 54

4.3 Fabrication........ 55

4.4 Experimental Results 57

4.4.1 Natural Frequency of the System........ 57

4.4.2 Self-Tuning Behavior of the System........ 62

4.4.3 Bandwidth of the System 66

4.4.4 Real Time Amplitude - Self Tuning 68

CHAPTER 5: CONCLUSION AND RECOMMENDATIONS............................. 71

5.1 Conclusion... 71

5.2 Recommendations 72

References 74

Appendix A 77

Appendix B 85

Appendix C 86

LIST OF FIGURES

Figure 2-1: Eco-Toxicology Effects of Various Compounds Found in Batteries (Melchor-Martínez et al., 2021) 21

Figure 2-2: Common Configuration for Vibration Energy Harvester (Sunithamani et al., 2020) 23

Figure 2-3: Experimental Setup of a Common Vibration Energy Harvester with Piezoelectric Element (D. Li, Han, Li, & Wang, 2017) 23

Figure 2-4: Magnet-Coil & Cantilever Setup Used to Extract Mechanical Energy from Vibration and Wind (Khan & Iqbal, 2018) 24

Figure 2-5: Micro Vibration Energy Harvester Based on Mass-Cantilever Design (Tang et al., 2018) 25

Figure 2-6 Power generated vs Frequency of Excitation Force. (Waterbury & Wright, 2013) 26

Figure 2-7: Multimodality via Multiple Cantilever Beams/Mass (Shahruz, 2006) 27

Figure 2-8 Output vs frequency from a Multimodal Array with 10 Piezo-Bimorph cantilevers. (Xue et al., 2008) 28

Figure 2-9: 3x Mass Cantilevers connected to 1 Piezoelectric Strip & the Output vs Frequency (X. Li et al., 2019). 29

Figure 2-10: Automatic Tuning Mechanism Showing Mass Movement When Frequency is Increased (Shin et al., 2020) 31

Figure 2-11: Self Tuning Mechanism Setup with Movable Mass Settling Near Vibration Node at a) 75Hz and b) 80Hz (Lan et al., 2021) 32

Figure 3-1: Execution Flow Chart 36

Figure 3-2: Exploded View of Testing Apparatus 38

Figure 3-3 Disc in Position 1 39

Figure 3-4 : Disc in Position 2 40

Figure 3-5: Position Reference Definition 40

Figure 3-6 : Side View of the Mass-Cantilever System Showing Gap 41

Figure 3-7: Drilling a Hole on the Cantilever Beam for the Asymmetrical Disc 42

Figure 3-8: Rotary Pipe Cutter Used to Cut the Spacer.. 43

Figure 3-9: Spacer Being Cut by the Rotary Pipe Cutter.. 43

Figure 3-10: Completed Spacer.. 44

Figure 3-11: Planned Holes on the 36mm Washer... 44

Figure 3-12: 4x Holes Being Drilled Using a Bench Drill 45

Figure 3-13: 4 x Holes Joined Using a Round File to Create the Groove 45

Figure 3-14: Asymmetrical Disc Formed After 4 x Holes Are Joined Together.......... 46

Figure 3-15: Installation of Testing Apparatus on top of TiraVib™ Shaker................ 47

Figure 3-16: Position of IEPE Accelerometer #1 on the Cantilever Beam 47

Figure 3-17: Power Amplifier Used to Drive TiraVib Shaker.................................... 48

Figure 3-18: Location of IEPE Accelerometer #2.. 48

Figure 3-19: Small Hammer Used to Deliver an Impulse to the System...................... 50

Figure 3-20: Hammer delivering an Impulse to the System 50

Figure 3-21: Laser Displacement Sensor Measuring Displacement at Tip of Bolt........ 52

Figure 4-1: Normalized Amplitude Response vs Frequency from EMA Analysis with the Rotating Mass Locked in 3 Positions 57

Figure 4-2: Amplitude Response at 0˚. Repeated 3 Times 59

Figure 4-3: Amplitude Response at 90˚. Repeated 3 Times 59

Figure 4-4: Amplitude Response at 180˚. Repeated 3 Times 60

Figure 4-5: Amplitude Response for all 3 Positions. First Trial 60

Figure 4-6: Amplitude Response for all 3 Positions. Second Trial.............................. 61

Figure 4-7: Amplitude Response for all 3 Positions. Third Trial................................. 61

Figure 4-8: Disc Final Settled Position vs Excitation Frequency................................. 62

Figure 4-9: Cantilever Locked at One End, At High Amplitudes, the Mass at the Tip Moves in an Arc 65

Figure 4-10: Cantilever Locked at Both Ends. At High Amplitudes, the Mass Moves in a Straight Line. 65

Figure 4-11: Bandwidth of Testing Apparatus compared to Bandwidth at 0˚ Position . 66

Figure 4-12: Definition and Improvement in Bandwidth 68

Figure 4-13: Real Time Amplitude at 39Hz. Disc Initial Position = 180˚..................... 69

Figure 4-14: Real Time Amplitude at 49Hz. Disc Initial Position = 0˚......................... 70

Figure 5-1: A Passive Device that Converts Vibration Motion into Rotary Motion. (Altshuler et al., 2013) 73

LIST OF TABLES

Table 1: Specifications of the Self-Tuning Mass-Cantilever System 55

Table 2 : Position of Rotating Disc VS Natural Frequency 58

Table 3: Acceleration Values of Disc Locked at 0˚ vs Self Tuning. 66

Table 4: Raw Result From Experimental Modal Analysis Conducted......................... 77

Table 5: First Trial Frequency Sweep at 3 Different Disc Positions 82

Table 6: Second Trial Frequency Sweep at 3 Different Disc Positions........................ 83

Table 7: Third Trial Frequency Sweep at 3 Different Disc Positions 84

Table 8: Settled Disc Position vs Frequency of Excitation.. 85

LIST OF SYMBOLS AND ABBREVIATIONS

EMA	:	Experimental Modal Analysis
RMS	:	Root Mean Square
IEPE	:	Integrated Electronics Piezo Electric
G	:	Gravity
HSS	:	High Speed Steel
MEMS	:	Micro Electro-Mechanical Systems
WSN	:	Wireless Sensor Networks

LIST OF APPENDICES

Appendix A: Experimental Data- Natural Frequency of Vibration Harvester 76

Appendix B : Self Tuning Behavior of Vibration Harvester 84

Appendix C: Bandwidth Of Vibration Harvester 85

CHAPTER 1: INTRODUCTION

1.1 Background of the project

The development of low power electronics has made wireless remote sensors and Internet of Things devices possible. Since the power consumption of these devices are low, they are usually powered by primary batteries. However, for long term use of such devices, the batteries need to be replaced periodically due to their finite capacity and lifespan.

If the devices are operated in areas with ambient vibration such as those generated by rotational or reciprocating machines, this vibrational energy can be converted to electrical energy to power the devices. This eliminates the need to use and change the batteries, significantly reducing the cost of running these devices, more so if those devices are located at locations that are difficult or hazardous to access.

A vibration energy harvester is typically configured in the form of a mass-spring system. A common arrangement to achieve that is a tip mass suspended on a cantilever beam. Piezoelectric element is attached to the cantilever beam, converting bending strain on the beam when it vibrates to electrical energy. The piezoelectric element can be replaced with a magnet and coil with the magnet attached near the tip of the cantilever. This magnet is surrounded by stationary copper windings. The movement of the magnet inside this coil as the beam vibrates induces an electrical current in the coil due to Faraday's law of induction. This electrical energy in the form of AC is then rectified to DC as required to power the electronic devices.

1.2 Problem Statement

The amount of electrical power generated by a harvesting system depends on amplitude of vibration of the mass-spring system. On simple mass-spring systems such as a mass-cantilever system, high amplitudes are generated only when the excitation frequency is at the natural frequency of the system. The amplitude drops significantly once the excitation frequency moves away from the natural frequency of the system. Depending on the size of the mass-spring system, Waterbury and Wright (2013) demonstrated that this bandwidth can be as narrow as 1 Hz, significantly reducing the power harvested or produced by the system when the ambient frequency is not exactly matched to the natural frequency of the vibration harvesting device.

A vibration harvesting mechanism that can adjust its natural frequency mechanically and passively by itself to be closer to the frequency of ambient vibration in both directions (increase in frequency and decrease in frequency) will have a wider operational bandwidth. This means it can produce more power to power required devices even when the frequency of the ambient vibration is not exactly matched with the natural frequency of the vibration harvesting device.

1.3 Objectives

This research aims to study the self-tuning behavior of a cantilever beam with a freely rotating asymmetrical disc attached at the tip of the cantilever.

(i) To design a novel passive self-tuning vibration harvesting device

(ii) To fabricate a working multimodal passive self-tuning vibration energy harvesting device

(iii) To experimentally investigate the tuning behavior of the device with respect to excitation frequencies

1.4 Scope of the work

(i) A novel multimodal self-tuning mass-cantilever system with a rotating asymmetrical mass is designed and fabricated.

(ii) The natural frequencies of the self-tuning system is determined experimentally

(iii) Determination of the self-tuning behavior & bandwidth of the system

The focus of this study is on the self-tuning behavior of a multimodal vibration harvesting device. Therefore, in defining the characteristics of the beam vs excitation frequency in this study, only the amplitude of acceleration and displacement is investigated in this study. When a piezo element is bonded on the cantilever, it would be expected that higher amplitude would generate larger bending strain on the cantilever, which induces higher electrical potential across the piezo element. The same applies for magnet-coil system, where higher amplitudes are associated with higher velocities, which would cause a larger rate of change in magnetic flux that would induce a larger current in the coil. A review on those systems can be found in Section 2.3.

CHAPTER 2: LITERATURE REVIEW

2.1 Energy harvesting systems and their applications

Energy Harvesting Systems are defined in this literature review as systems that are designed to convert, harness or harvest ambient energies such as heat, light, wind and mechanical vibration into electrical energy directly (Staaf, Köhler, Soeiro, Lundgren, & Enoksson, 2015).

Direct conversion of light to electricity has been the most successfully implemented, as proven by the widespread use and deployment of solar panels. The same can be said for wind energy harvesting and the widespread deployment of wind turbines. The large scale deployment of these 2 technologies alone is responsible for 32.6% of the world's renewable electricity production in 2020 (IEA, 2020).

Devices utilizing the thermoelectric effect or Seebeck effect are known to generate an electrical current when subjected to a temperature difference between the hot and cold side, but the power produced is typically very low, in the order of μW to mW (Park et al., 2019). The same goes for Vibration Harvesting Devices which are discussed in detail in Section 2.3. However, on this scale of power generation, there are other developments and requirements in the area of sensor networks that made energy harvesting of heat and vibration, viable.

Traditional sensor networks typically consist of sensors that are connected to an acquisition system via wires. Both the electrical power to power the sensors and the electrical signal from the sensors to the acquisition system travels through these wires. Depending on how far those sensors are & the numbers of sensors in the system, the amount of wires can be astounding. With the advent of wireless information systems, the information from the sensors can now be transmitted wirelessly. WSN or Wireless Sensor Networks are attracting significant research over the past 10 years, research that encompasses areas such as sensor designs, power consumption optimization, wireless communications protocol, data transmission and security, wireless topologies, etc (Zhang, 2018). However, these devices still have to be powered, and chemical batteries are the default method to power those devices.

Waterbury and Wright (2013) states that modern wireless sensors node typically require around 100μW – 1mW to operate. This is within the range of power produced by Energy Harvesting Systems highlighted in this Literature Review. Therefore, using Energy Harvesting Systems such as Vibration Energy Harvesting System to replace chemical batteries is a real possibility, and this area of study has attracted significant research interest lately (Sunithamani, Rooban, Nalinashini, & Rajasekhar, 2020).

2.2 Limitations of batteries

While battery technologies have progressed significantly over the past 50 years, there are still limitations to them that cause their applications in wireless sensor nodes to be less than ideal. At its most basic level, batteries are divided into 2 types, namely Primary Batteries, that are single use and unable to be recharged or re-energized by reversed current flow, and Secondary batteries, which are batteries that can be recharged by reversed current flow.

Primary batteries, such as alkaline cells, silver oxide cells, and Lithium cells form the backbone of energy supply for most electronic devices, including wireless sensor nodes.

These batteries are single use and disposable. The main issues with these batteries are finite capacity and environmental impact during disposal.

The typical capacity of primary Lithium batteries are in 400 Wh/kg range (Chen, Dai, & Tang, 2020). This means, a 10 gram lithium battery would have a capacity of 4Wh. A wireless sensor node that consumes 1mW of power as highlighted by Waterbury and Wright (2013) would drain that battery completely in about 4000 hours, or about 5 months. After that, the battery would need to be replaced physically. This act of replacing said battery might be a simple process, but if the sensors are placed in locations that are difficult or hazardous to access, and/or there are many sensor nodes in the acquisition system, it poses a significant operational challenge. While there are power conserving modes in those devices such as the algorithm suggested by Cundeva-Blajer and Srbinovska (2018) and Sachan, Sharma, and Sehgal (2021), size limitations of wireless sensor nodes may cause the designer of those devices to use even smaller batteries (<10g) which would offset the improvements brought forth by low power consuming modes. In other words, low power consuming modes and power optimization algorithm may lengthen the lifespan of batteries, but they do not change the fact that battery capacities are still finite and a battery change is still required down the road.

Once the batteries are spent, they need to be replaced and disposed. In 2018, it is estimated that only 5% out of 345,000 tons of Lithium batteries are recycled (Melchor-Martínez et al., 2021). This means most of the batteries end up in landfill where chemicals with high eco-toxicity can potentially leak into the ground and groundwater, contaminating the environment and ecology. In their review of environmental impact of contaminants from battery waste, Melchor-Martínez et al. (2021) listed the eco-toxicological effects of various chemicals typically found in batteries, with biological effects such as oxidative stress caused by metal oxide compounds to disruptions to synthesis of nuclei acids caused by Lithium compounds.

Contaminant	Ecotoxicological effects
Cadmium	Intake by ingestion of contaminated food crops. Accumulation in the human body may cause kidney diseases Carcinogenic effects.
Cobalt	Adverse effects on biomass and on physiological activity in crops.
Copper	Intake by ingestion of contaminated food crops. Liver damage and gastric-related problems. Neurological complications.
Lead	Intake by ingestion of contaminated food crops. Negative effects on nervous systems, kidney and other organs. Cardiovascular diseases. Carcinogenic effects.
Lithium	Alterations in the development of invertebrates. Interference with nucleic acids synthesis. Accumulation in soil causes severe phytotoxicity.
Nickel	High oxidative stress in mammalian and terrestrial plant systems. Disruption of ion homeostasis.

Figure 2-1: Eco-Toxicology Effects of Various Compounds Found in Batteries (Melchor-Martínez et al., 2021)

Limitations such as finite capacity of primary batteries can partially be solved via the use of rechargeable batteries coupled to a power producing device such as solar panels. Vellucci et al. (2014) tested a Lithium Ion pack through hundreds of cycles, and clear capacity degradation is observed. Hence, the battery cycle lifespan is still finite and rechargeable batteries still share the same downside as primary batteries when disposed. In addition to that, the size and position limitations of certain wireless sensor nodes such as those designed for Structural Health Monitoring on the skin of aircraft by Fu, Sharif-Khodaei, and Aliabadi (2019) do not allow such arrangements with solar panels to happen.

In view of the limitations of batteries in powering Wireless Sensor Nodes, the use of Energy Harvesting Systems that harvest energy directly from the environment in which the Sensor Nodes operate has the potential to replace chemical batteries in that application, potentially avoiding the limitations of batteries listed above.

2.3 Vibration energy harvesting system

Energy consumption of small electronics devices have reduced significantly over the last 10 years. This has attracted significant research interest in the field of Vibration Energy Harvesters, where the energy produced by them is now sufficient to power small electronics devices such as distributed wireless sensor nodes and replace conventional chemical batteries traditionally used to power those devices (X. Li, Yu, Upadrashta, & Yang, 2019). This reduces environmental pollution caused by those batteries that need to be replaced and disposed once depleted.

The purpose of Vibration Energy Harvesting system is to extract usable electrical energy from ambient vibrations surrounding it. Sunithamani et al. (2020) discussed about the most common configuration for Vibration Energy Harvester, which consists of a cantilever beam with piezoelectric elements bonded to the cantilever beam. The fixed end is fixed to the point where vibration is expected to be harvested, such as the skin of an aircraft in the system designed by Fu et al. (2019) or the body of a piece of rotating machinery in the system tested by Shin et al. (2020). The proof mass, or tip mass is freely suspended. External vibration at the fixed end causes the proof mass to vibrate as well. As that proof mass vibrates up and down relative to the fixed end, the cantilever is subjected to periodic bending. This periodic bending strains the piezoelectric layer that is bonded or deposited to the cantilever, which generates a potential difference due to the piezoelectric effect. Since this electricity is generated from the periodic straining of the cantilever beam, it is in the form of Alternating Current, which needs to be rectified to Direct Current before being used by remote sensors.

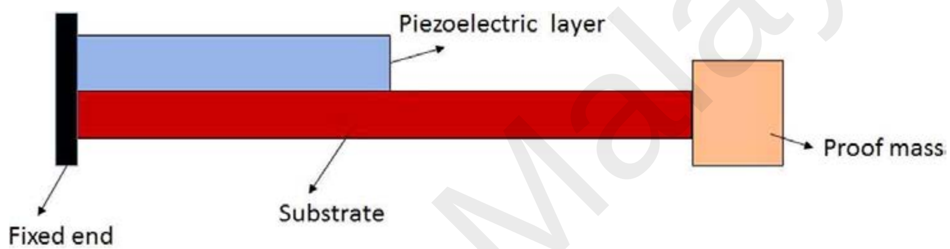

Figure 2-2: Common Configuration for Vibration Energy Harvester (Sunithamani et al., 2020)

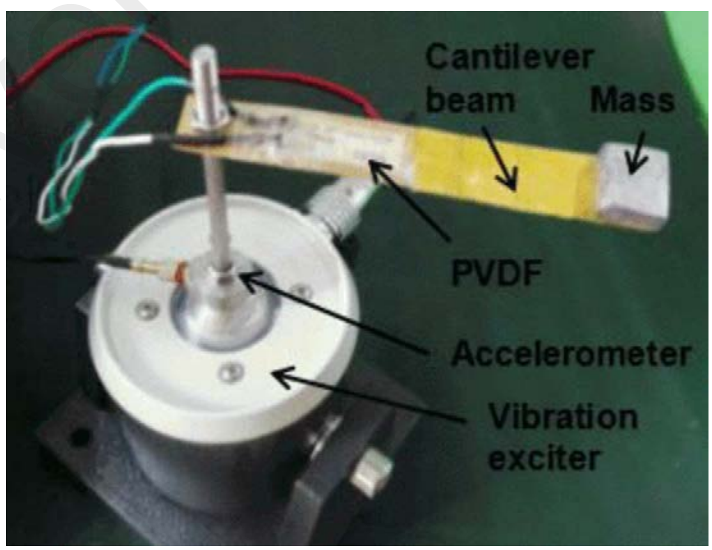

Figure 2-3: Experimental Setup of a Common Vibration Energy Harvester with Piezoelectric Element (D. Li, Han, Li, & Wang, 2017)

A similar mass-cantilever setup is employed by Khan and Iqbal (2018) in their prototype Vibration Energy Harvester. It is designed to extract energy from both vibrations and wind around bridges from passing traffic in order to power wireless sensor nodes that are used to monitor the structural health of the bridge. However rather than using piezoelectric elements, a magnet coil system is employed to convert the mechanical energy of vibration into electrical current. When the tip mass is vibrating, the magnet placed at the tip of the cantilever as shown in Figure 2-4 will move and vibrate relative to the coil. This movement of the magnetic field as seen by the coil induces a current in the coil according to the Faraday's Law of Induction. The system shown in Figure 2-4 was able to generate 354.51μW of electrical power when subjected to a vibration of 0.4g at the natural frequency of the device at 3.6 Hz.

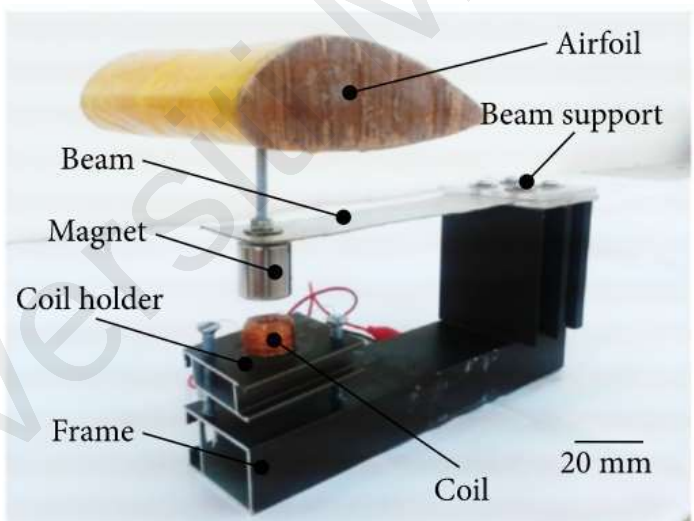

Figure 2-4: Magnet-Coil & Cantilever Setup Used to Extract Mechanical Energy from Vibration and Wind (Khan & Iqbal, 2018)

These Vibration Energy Harvesters come in various sizes. Tang et al. (2018) built a Micro Vibration Energy Harvester based on Mass-Cantilever with a surface area of only about 1 cm^2. It is able to generate 304μW of electrical power when subjected to a vibration at 0.5g with a frequency of 126Hz, which is the natural frequency of the mass-cantilever system. The tip mass is made out of Tungsten that is glued to a stainless steel cantilever that is fabricated using chemical etching process. Piezoelectric material is then deposited on the cantilever using Aerosol Deposition Method.

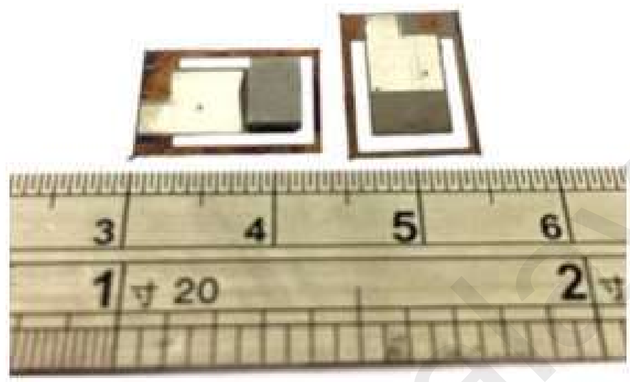

Figure 2-5: Micro Vibration Energy Harvester Based on Mass-Cantilever Design (Tang et al., 2018)

With piezoelectric based Vibration Energy Harvester, the amount of power produced is dependent on the amount of strain on the piezoelectric element. The same goes for magnet-coil system, where power produced is dependent on the rate of change in magnetic flux as "seen" by the coil. This 2 will only be large when the amplitude of vibration is large, and the only way the amplitude can be large is when the external excitation frequency is exactly matched with the natural frequency of the device, a phenomena known as resonance.

2.4 Narrow Frequency Band

From basic understanding of resonance, it is well documented that resonance happens at a very narrow frequency band (Hibbeler, 2016). For a simple fixed mass-spring vibration harvesting system, Waterbury and Wright (2013) demonstrated that the bandwidth could be as narrow as 1 Hz before the power output drops below 50% of maximum power output at resonance as shown in Figure 2.1. Similar observation is also noted by Khan and Iqbal (2018) and Tang et al. (2018) in their Vibration Harvesting Systems discussed in Section 2.3.

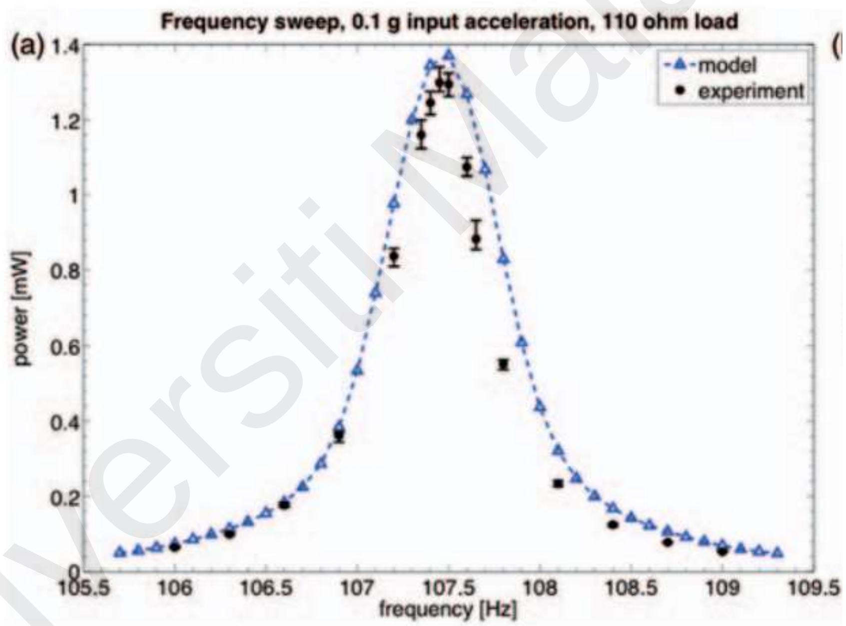

Figure 2-6 Power generated vs Frequency of Excitation Force. (Waterbury & Wright, 2013)

2.5 Multimodality

There are several ways to address the narrow frequency band of a simple mass-spring vibration energy harvester system. 2 methods are explored here, which are Multiple Stacked Systems and Self-Tuning Systems.

2.5.1 Multiple Stacked Systems

Yildirim, Ghayesh, Li, and Alici (2017) discussed about Multiple Degrees of Freedom (MDOF) systems, where multiple masses are placed in the system. The presence of multiple masses creates a system with multiple natural frequencies. Perez et al. (2020) demonstrated that a 2 Degrees of Freedom system has a wider bandwidth and thus, able to generate higher power compared to a 1 Degree of Freedom system due to the presence of a 2nd natural frequency. Yildirim et al. (2017) also discussed about Multi Modal arrays, where there are multiple mass-spring systems, each tuned to a different natural frequencies, in which the electrical power outputs from each system is added up electrically to the final power produced.

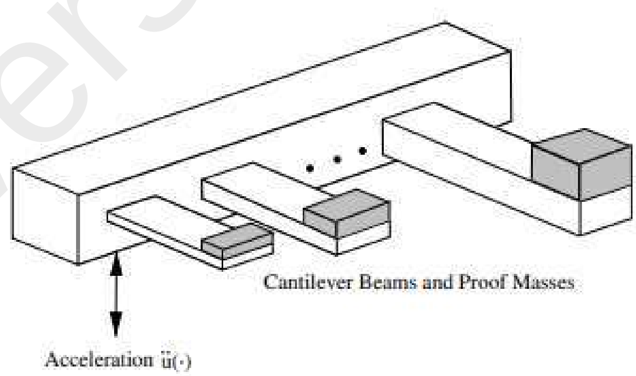

Figure 2-7: Multimodality via Multiple Cantilever Beams/Mass (Shahruz, 2006)

Xue, Hu, and Wang (2008) demonstrated that it is possible to achieve multimodality this way by having multiple piezo-electric bimorphs cantilevers with dimensions that has different natural frequencies, and connecting them electrically in series. With 10 such Piezo-electric bimorphs, a wide bandwidth was created. X. Li et al. (2019) improved on this concept by building a device with 3 cantilevers with different tip masses but they are attached to the same piezoelectric strip. This eliminates the complexity when connecting several piezoelectric elements together electrically, with the need to match impedance and such which is outside the scope of this literature review.

Both Xue et al. (2008) and X. Li et al. (2019) setup achieve a bandwidth that is wider compared to a single mass-cantilever system as shown in Figure 2-8 and Figure 2-9. However, in X. Li et al. (2019) setup, the resonant frequencies of the 3 cantilever beams are probably spaced too far from one another. That is why although multimodality is achieved, there are obvious gaps in response in Figure 2-9.

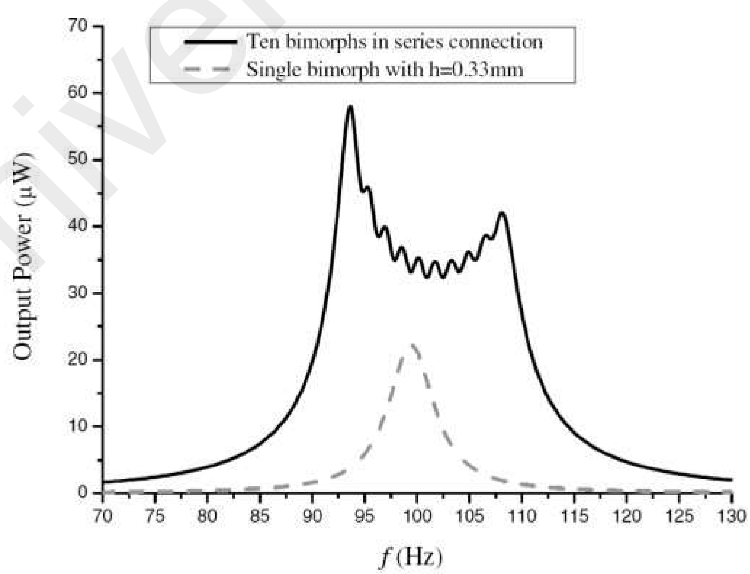

Figure 2-8 Output vs frequency from a Multimodal Array with 10 Piezo-Bimorph cantilevers. (Xue et al., 2008)

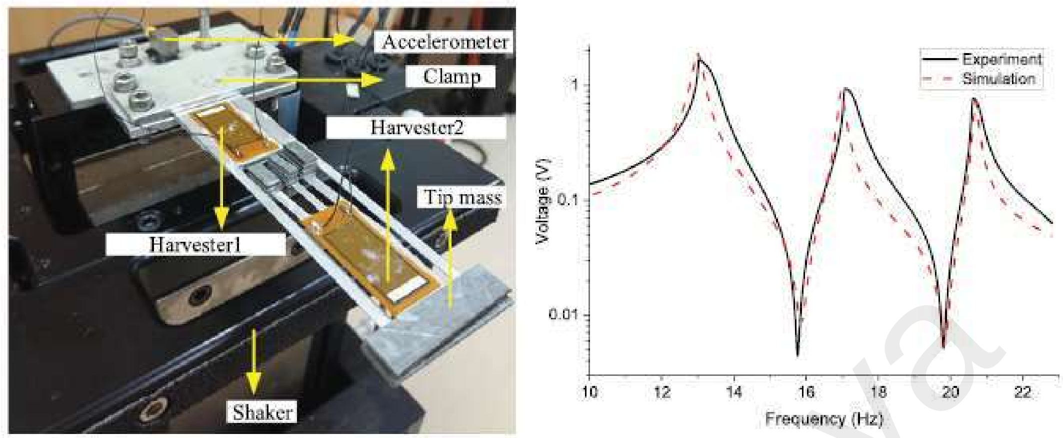

Figure 2-9: 3x Mass Cantilevers connected to 1 Piezoelectric Strip & the Output vs Frequency (X. Li et al., 2019).

Both Multimodal arrays and MDOF systems basically stacks up the response from each natural frequencies, and depending on the number of Degrees of Freedom or size of the arrays, the size and complexity of the system can increase significantly. However, it made wideband energy harvesting possible with existing technologies and methods.

2.5.2 Self-Tuning Systems

Another method is via the use of self-tuning systems. Self-tuning is defined here as systems that has only a single natural frequency at a given time, but that natural frequency can be adjusted by itself, by changing systems parameters, so that the natural frequency can match or be closer to the frequency of external excitation.

Zhu, Tudor, and Beeby (2010) and D. Li et al. (2017) shows that for a tip mass-cantilever system, the natural frequency of the cantilever beam depends on the position of the mass and stiffness of the cantilever. If stiffness of the beam can be increased, the natural frequency of the system can be increased as well and vice versa. Lallart, Anton, and Inman (2010) demonstrated this by adjusting the beam stiffness using a piezoelectric element bonded to the beam. By controlling the voltage applied to the piezoelectric element, the stiffness of the beam can be varied to match the excitation frequency. However, in this application, controlling the stiffness of the beam consumes a large part of energy generated by the energy harvesting system. The energy produced can even be negative, where power generated is less than power required to control the stiffness of the beam.

If a method can be devised to move the mass on the cantilever, self-tuning can also be achieved. There are 2 ways to move this mass. Passive and active. An active method relies on sensors and actuators such as stepper motors to move the mass. Yildirim et al. (2017) and Bukhari, Malla, Kim, Barry, and Zuo (2020) discussed that this can be unrealistic because the power generated by most vibration harvesting system is smaller than the power required to operate actuators, sensors and the associated control systems to move the mass on the cantilever. Hence, a passive mechanism that is able to move the mass mechanically by itself would be required for most systems to be viable.

Shin et al. (2020) built a system that changes the position of the mass relative to a thin clamped-clamped beam passively as method to achieve passive self-tuning. When the excitation frequency is not at its natural frequency, a well-tuned gap between the mass and beam allows the mass to slowly slide along the beam towards the support until it reaches the point where the natural frequency of the system matches the excitation frequency. At this point, resonance occurs and amplitude increases significantly. It is demonstrated that the sliding mass stays in place during resonance. When the excitation frequency is increased, the mass will now move to seek a new resonant position.

Similar work is done by Lan, Chen, Hu, Liao, and Qin (2021), but rather than using a clamped-clamped beam, they use a cantilever with a free end, but unlike Shin et al. (2020) setup, the beam is excited at 2nd vibration mode. With this mode, the mass moves to seek the nodal point of the beam as shown in Figure 2-11, settling close to it.

However, in Shin et al. (2020) setup, it is not demonstrated in the literature that if the excitation frequency is decreased, the sliding mass will self-tune accordingly.

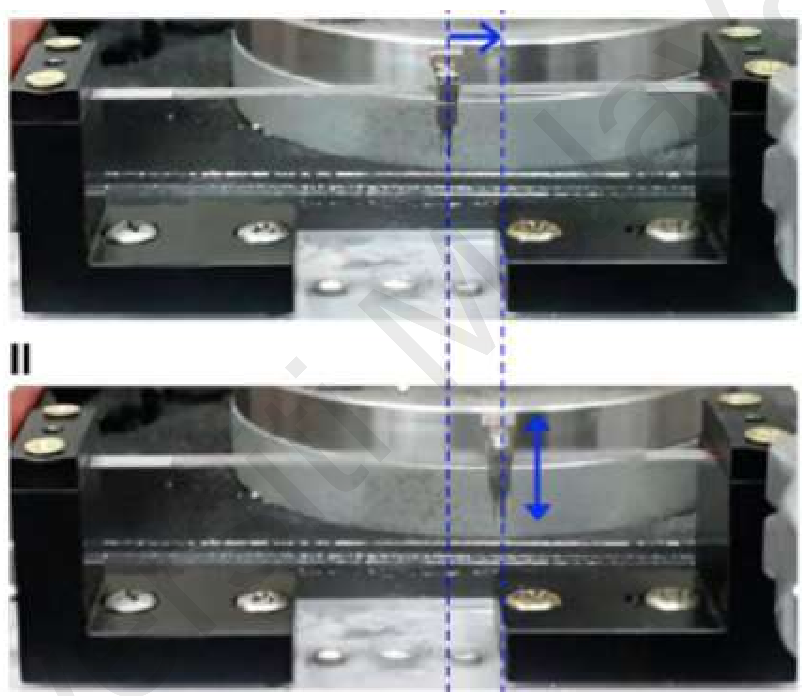

Figure 2-10: Automatic Tuning Mechanism Showing Mass Movement When Frequency is Increased (Shin et al., 2020)

The same goes for the setup of Lan et al. (2021). During literature review, the system's response with decreasing excitation frequency is not demonstrated in the literature

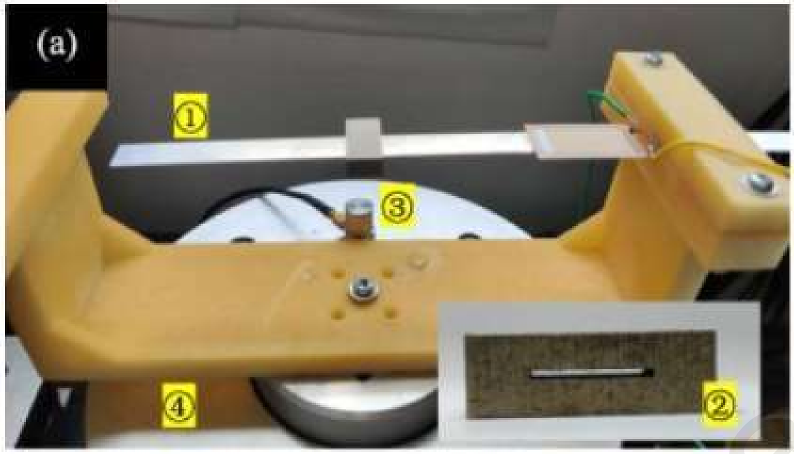

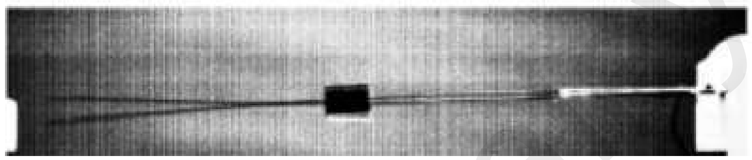

(a)

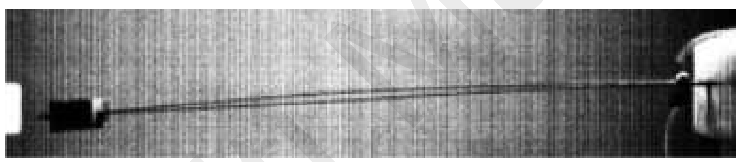

(b)

Figure 2-11: Self Tuning Mechanism Setup with Movable Mass Settling Near Vibration Node at a) 75Hz and b) 80Hz (Lan et al., 2021)

2.6 Literature Review Summary

The miniaturization and reduced power consumptions of modern electronics has made the power consumption of Wireless Sensor Nodes low enough to be powered by Vibration Energy Harvesters, potentially replacing batteries. Vibration Energy Harvesters are energy harvesters that harvest energy from ambient vibrations surrounding the harvester. Due to well understood resonance phenomena and the way the vibration harvesters are set up, vibration energy harvesters are only effective when the ambient vibrations are at the natural frequency of the harvester. Very little electrical power is produced in off resonance conditions. There are several methods currently under research that attempts to address this. Multiple Energy Harvesters, each tuned to a slightly different natural frequency is the most direct method at the moment. However, having multiple harvesters adds complexity to the setup. Another method is self-tuning. Such systems have only 1 natural frequency at a given time, but the natural frequency can be altered, either actively or passively. Active tuning requires the use of sensors, actuators and control systems to tune the natural frequency, and would typically consumes more power than a vibration energy harvester can produce. Passive systems changes the natural frequency mechanically without external intervention and 2 most recent work on this are discussed in this literature review. In the 2 passive systems reviewed, the literature review shows that it would self-tune when the excitation frequency is increased. However, self-tuning with decreasing excitation frequency is not demonstrated in the literature reviewed by the author. Thus, this research attempts a different method to achieve passive self-tuning, with the ability to self-tune when the excitation frequency is both increasing and decreasing.

CHAPTER 3: METHODOLOGY

3.1 Introduction

This chapter highlights the methodology employed to achieve the objectives stated in Section 1.3. It covers the following, arranged as per the objectives of this research. Section 3.2 provides a big picture overview of the entire research, Section 3.3 covers the design methodology and concepts behind the design, Section 3.4 covers the methodology for fabrication and Section 3.5 covers the methodologies employed to test the Fabricated Vibration Harvester.

3.2 Execution flow.

This research can be divided into several distinct phases according to Figure 3-1. The phases are: 1) Define the Problem & Literature Review on the State of the Art, 2) Design & Fabricate Self Tuning Vibration Harvester System, 3) Assemble & Test Vibration Harvesting System, 4) Perform Experimental Modal Analysis (EMA) to Determine the Natural Frequency of Vibration Harvesting System, 5) Test Vibration Amplitude Vs Excitation in Fixed Position & In Self Tuning Mode, 6) Real Time Measurement of Vibration Amplitude During Self-Tuning, and 7) Data Analysis. The summary of each phase is discussed below.

This research is initiated by conducting literature review on techniques that is done by other researchers and the tuning behavior of their systems. Some limitations were found, namely on the ability to tune itself when the excitation frequency is decreased. This Literature Review is documented in CHAPTER 2:

A self-tuning mass-cantilever system is designed and fabricated with the expectation that it would self-tune when subjected to increasing and decreasing excitation frequencies. The design and fabrication methodology is documented in Section 3.3 and 3.4 respectively.

Once the Vibration Harvesting System is fabricated, it is assembled and tested to ensure it would have the desired tuning behavior prior to starting the experiments below. The assembly methodology is documented in Section 3.4.5.

Next step would be to perform Experimental Modal Analysis to determine the natural frequency range of the Vibration Energy Harvester. The methodology and a summary of what is EMA are documented in Section 3.5.1

To do this, the self-tuning behavior of the Vibration Harvester vs excitation frequency is determined first. The methodology is documented in Section 3.5.2. With that done, the bandwidth when the Vibration Harvesting System is allowed to self-tune is determined and compared with the bandwidth when it is locked. The methodology for this is documented in Section 3.5.3.

The increase in amplitude as the system tunes itself with respect to time is demonstrated in this section via the use of Laser Displacement Sensor. This test is also done in the direction of increasing excitation frequency and decreasing excitation frequency. The methodology is documented in Section 3.5.4

The results obtained in this research is collated and discussed. This is covered in Chapter 4.

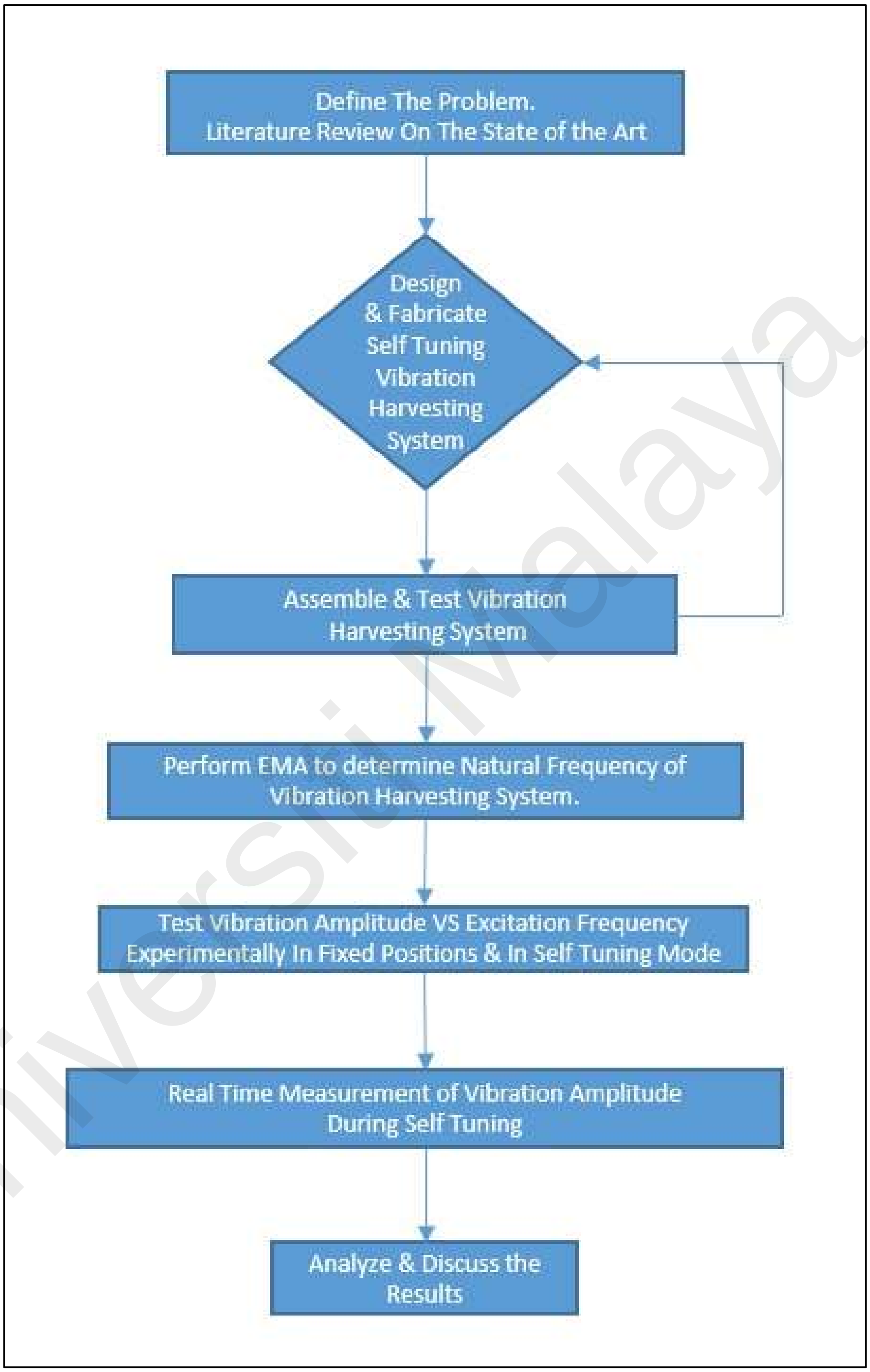

Figure 3-1: Execution Flow Chart

3.3 Self-Tuning Vibration Harvester Design

The vibration harvester is designed based on the following observations and considerations.

i) A loosely supported disc/shaft is known to rotate when it is subjected to external vibrations. This effect is commonly observed with mechanical threaded fasteners, in which vibration is known to cause the fasteners to loosen over time. Cyanoacrylate locking compounds or several other mechanical locking methods are typically used to prevent the threaded fasteners from loosening when subjected to external vibration in the industry.

ii) The rotary position of an asymmetrical disc affects the mass distribution of the disc. If this asymmetrical disc is placed at the end of a cantilever beam, the mass distribution of the disc on the beam is a function of the rotary position of the disc relative to the cantilever beam. This in turns alters the natural frequency of the mass-cantilever system.

iii) The rotation of the asymmetrical disc can happen in both directions, with no end stops. Thus the system is expected to self-tune when the excitation frequency is increasing or decreasing.

Since vibration is known to rotate a loosely supported disc, and the natural frequency of a mass-cantilever system is affected by the mass distribution of a loosely supported asymmetrical disc placed near the tip of the cantilever beam, this study aims to study the combined effects of those 2 observations to determine if they are able to cause some sort of self-tuning behavior that can widen the bandwidth of vibration harvesting devices.

The final design consists of a freely rotating symmetrical disc as shown in Figure 3-2.

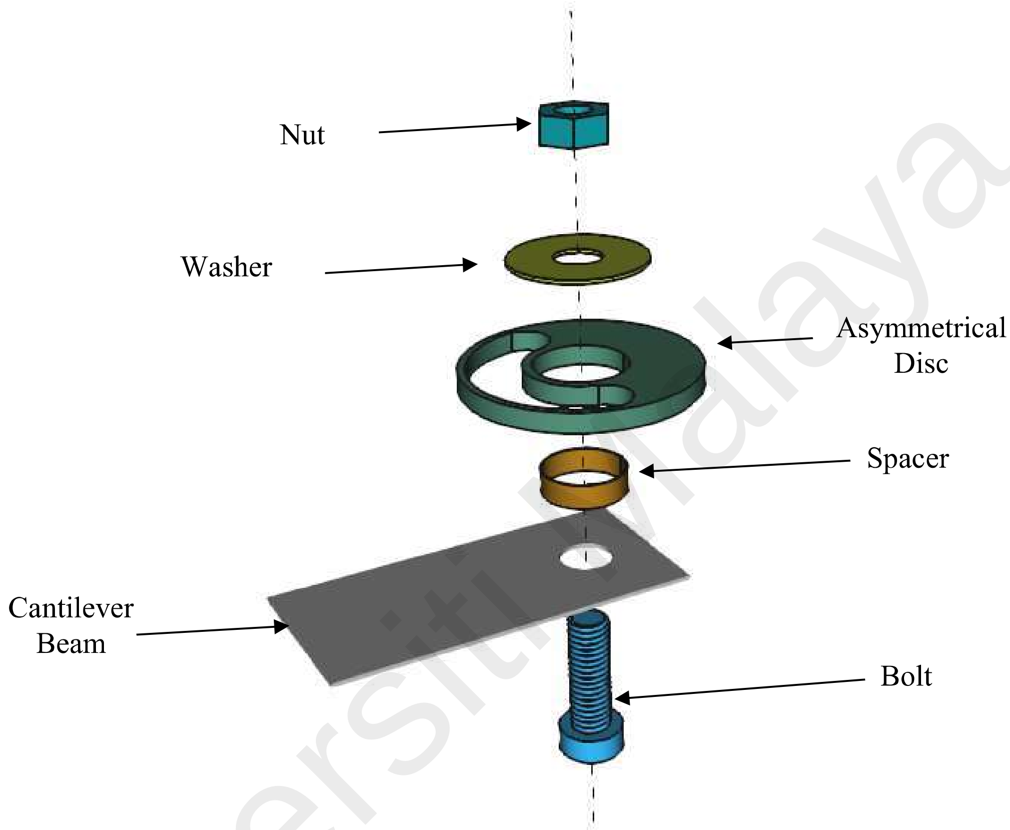

Figure 3-2: Exploded View of Testing Apparatus

The Spacer is 0.7mm thicker than the Asymmetrical Disc. Thus when the Bolt and Nut is locked, the washer engages the top of the Spacer rather than the Asymmetrical Disc, allowing the disc to rotate freely, yet with an axial displacement that is limited to 0.7mm as shown in Figure 3-6. This gap allows the disc to rotate with vibration. The OD of the Spacer is also smaller than the ID of the Asymmetrical Disc. The entire Testing Apparatus is clamped to a support as shown in Figure 3-16 . A small amount of solid lubricant (powdered graphite) is also applied to the bottom of the asymmetrical disc.

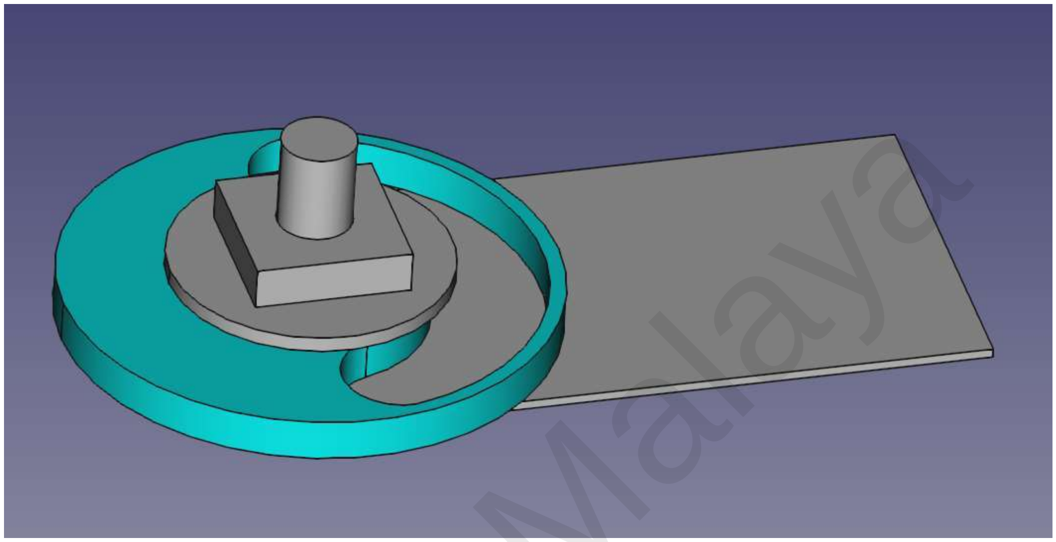

Figure 3-3 Disc in Position 1

Due to the cut-out, the disc becomes asymmetrical. Thus the rotary position of the disc alters the mass distribution on the cantilever. This in turn alters the natural frequency of the mass-cantilever system. The purpose of using a rotating disc to alter mass distribution on a beam is to allow frequency selection or self-tuning behavior to occur in both directions, i.e. in the direction of increasing excitation frequency and decreasing excitation frequency.

When the disc is in position 1 as shown in Figure 3-3, the mass is distributed towards the tip of the beam, and a lower natural frequency is expected.

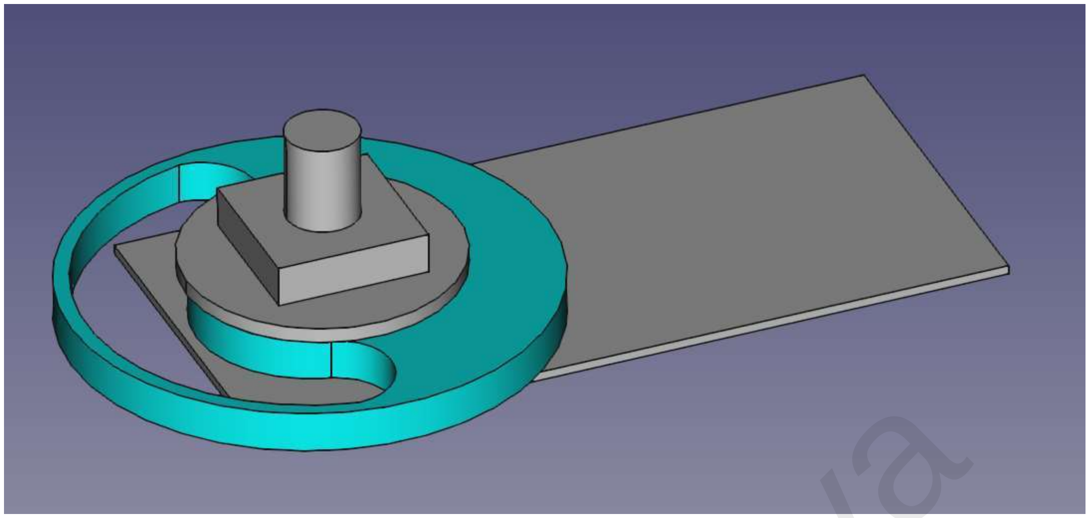

Figure 3-4 : Disc in Position 2

Likewise, when the disc is in position 2 as shown in Figure 3-4, the mass is distributed towards the center of the beam, and a higher natural frequency is expected. Therefore, the natural frequency of the system is a function of angular position of the disc.

The angular position of the mass relative to the cantilever is defined in Figure 3-5. Actual measurements are done by a protractor.

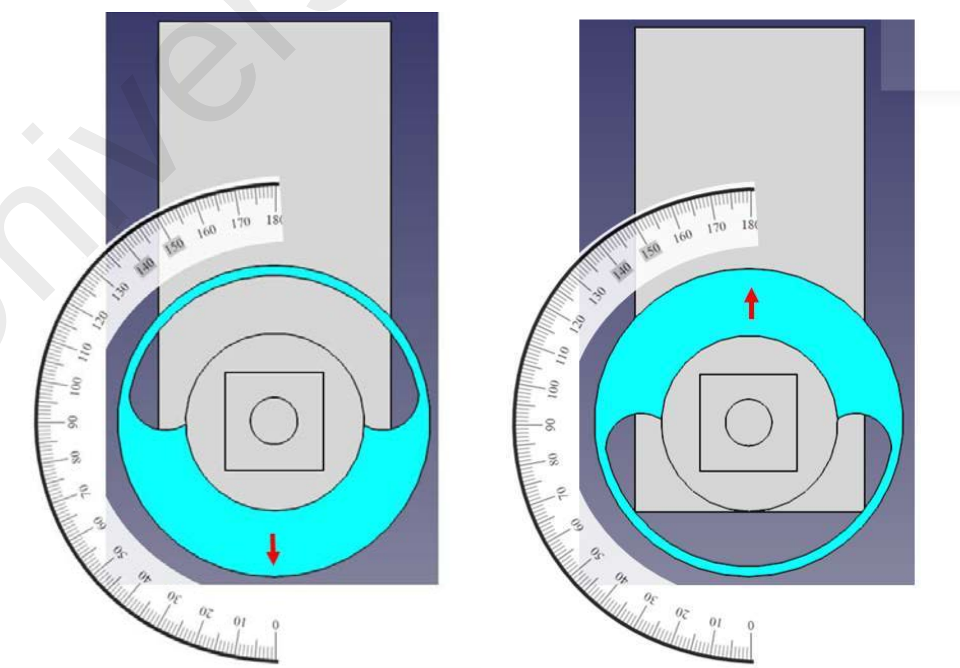

Figure 3-5: Position Reference Definition

The disc is free to rotate with respect to the cantilever, with a vertical gap of 0.7mm. This gap is important, and significant trial and error was required to fine tune this gap such that the self-tuning behavior has the effect of improving the bandwidth of the testing apparatus.

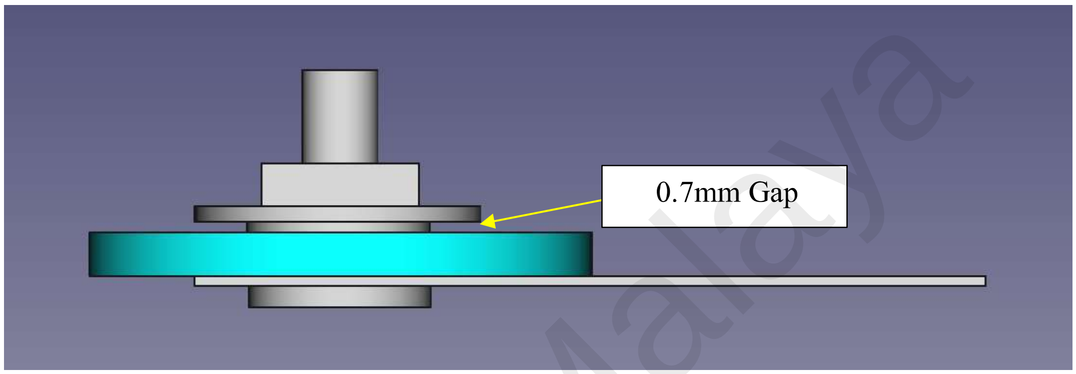

Figure 3-6 : Side View of the Mass-Cantilever System Showing Gap

3.4 Fabrication

From Figure 3-2, the testing apparatus consists of the following main parts,

i) Cantilever Beam

ii) Spacer

iii) Asymmetrical Disc

iv) Bolt-Nut-Washer

3.4.1 Cantilever Beam

The cantilever beam is made out of a standard issue 26mm width steel metal ruler that is widely available from stationary shops. The metal ruler is cut at 150 mm length. A 6mm hole is drilled into the middle of the cantilever beam 11mm from the edge of the beam using a bench drill and a 6mm HSS drill bit, set at 1000rpm. A block of wood is placed underneath the beam to allow the drill bit to drill through the beam. The burr at the hole is then smoothened off using a round file.

Figure 3-7: Drilling a Hole on the Cantilever Beam for the Asymmetrical Disc

3.4.2 Spacer

The spacer is made out of a 14mm stainless steel tube with 0.5mm wall thickness. It is cut using a rotary pipe cutter to a rough height of 4 mm as shown in Figure 3-9. It is then filed down to a height of 3.65mm as measured using a Vernier caliper.

Figure 3-8: Rotary Pipe Cutter Used to Cut the Spacer

Figure 3-9: Spacer Being Cut by the Rotary Pipe Cutter

Figure 3-10: Completed Spacer

3.4.3 Asymmetrical Disc

The asymmetrical Disc is made from a 36mm diameter steel plain washer with an inner diameter of 15mm. 4 x 6 mm holes are drilled as per Figure 3-11. Once the 4 holes are drilled, a round file is used to file off excess materials to join the 4 holes together as shown by the dashed line in Figure 3-11.

Figure 3-11: Planned Holes on the 36mm Washer

Figure 3-12: 4x Holes Being Drilled Using a Bench Drill

Figure 3-13: 4 x Holes Joined Using a Round File to Create the Groove

Figure 3-14: Asymmetrical Disc Formed After 4 x Holes Are Joined Together

3.4.4 Bolt-Nut-Washer

Standard M5 Bolt- Nut and 25mm steel washer are used for this purpose.

3.4.5 Assembly

The various parts are then put together as per Figure 3-2 and the bolt-nut tightened. The assembly is then clamped to an existing support found in UM Vibration Lab as shown in Figure 3-15 . The length of the unsupported beam is then adjusted to 55mm.

Figure 3-15: Installation of Testing Apparatus on top of TiraVib™ Shaker

Once the system is assembled, a small IEPE accelerometer is glued to the cantilever beam 15mm from the base support of the cantilever as shown in Figure 3-16.

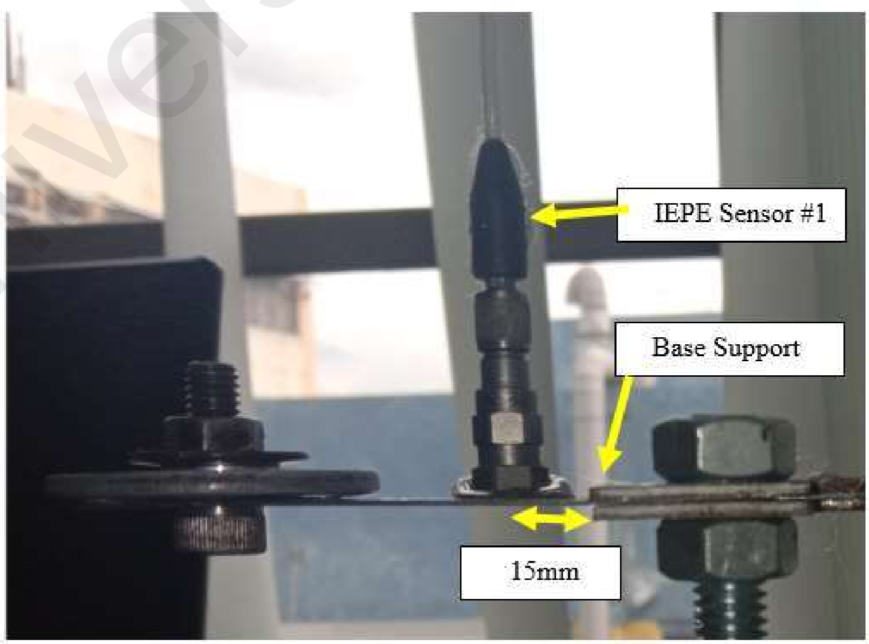

Figure 3-16: Position of IEPE Accelerometer #1 on the Cantilever Beam

The Testing Apparatus is then bolted to the top of a TiraVib™ shaker. Another IEPE sensor is attached to the base of the rig holding the cantilever as shown in Figure 3-18.

Figure 3-17: Power Amplifier Used to Drive TiraVib Shaker

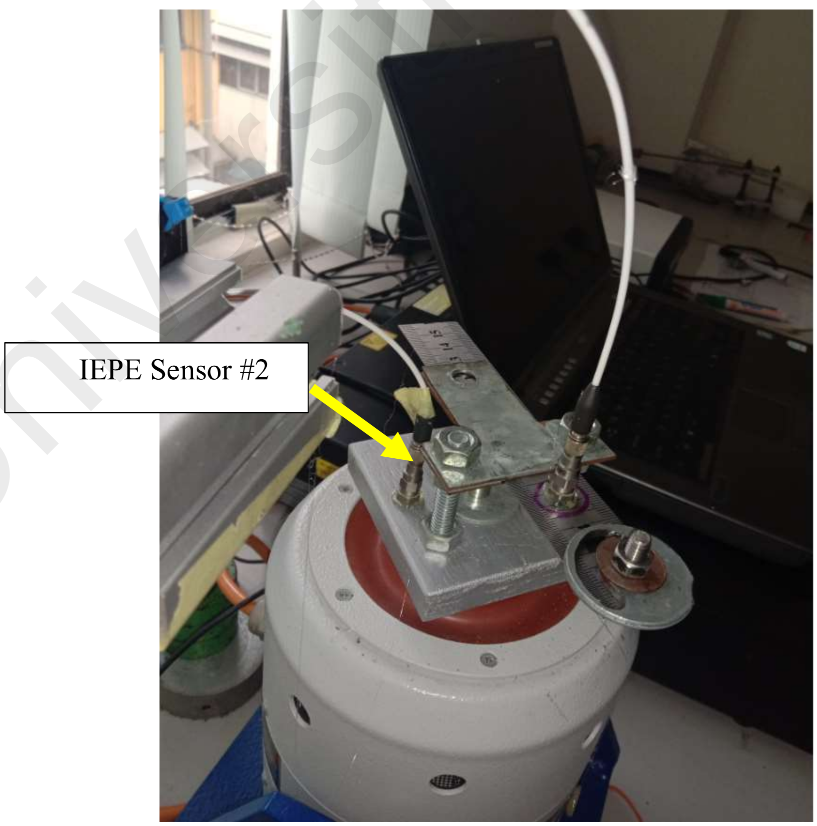

Figure 3-18: Location of IEPE Accelerometer #2

A pretest was conducted to test at what frequency the disc will rotate reliably. A frequency sweep from 20Hz – 80 Hz was conducted with 1 Hz interval with an input vibration at 2G-RMS. The frequency range at which the disc rotate reliably is noted and this forms the frequency range of interest for the rest of the experiments that follow.

3.5 Experiments to Determine Tuning Behavior

Now that the testing apparatus is fabricated and assembled, the next step is to test the tuning behavior of the testing apparatus. The process is divided into several steps, aptly named based on the system's behavior that is tested.

i) Determination of the Natural Frequency of the System

ii) Determination of the Self-Tuning Behavior of the System

iii) Determination of the Bandwidth of the System

iv) Real Time Self Tuning Behavior

3.5.1 Determination of the Natural Frequency of the System

The first part of the experiment is to obtain the natural frequency of the testing apparatus at various disc positions. Experimental Modal Analysis is conducted on the disc-cantilever setup.

In order to perform EMA, a small impulse is delivered to the system using a hammer. Since an impulse excites the beam at all frequencies, the beam will vibrate at its natural frequency upon impact. This transient vibration is picked up by IEPE accelerometer #1, and post processed using Fast Fourier Transform. This is all done using an In House Modal Testing software that is implemented on Labview. The natural frequency of the system is determined from the peak of the FFT spectrum. The natural frequencies at all 3 positions are presented in Figure 4-1.

Figure 3-19: Small Hammer Used to Deliver an Impulse to the System

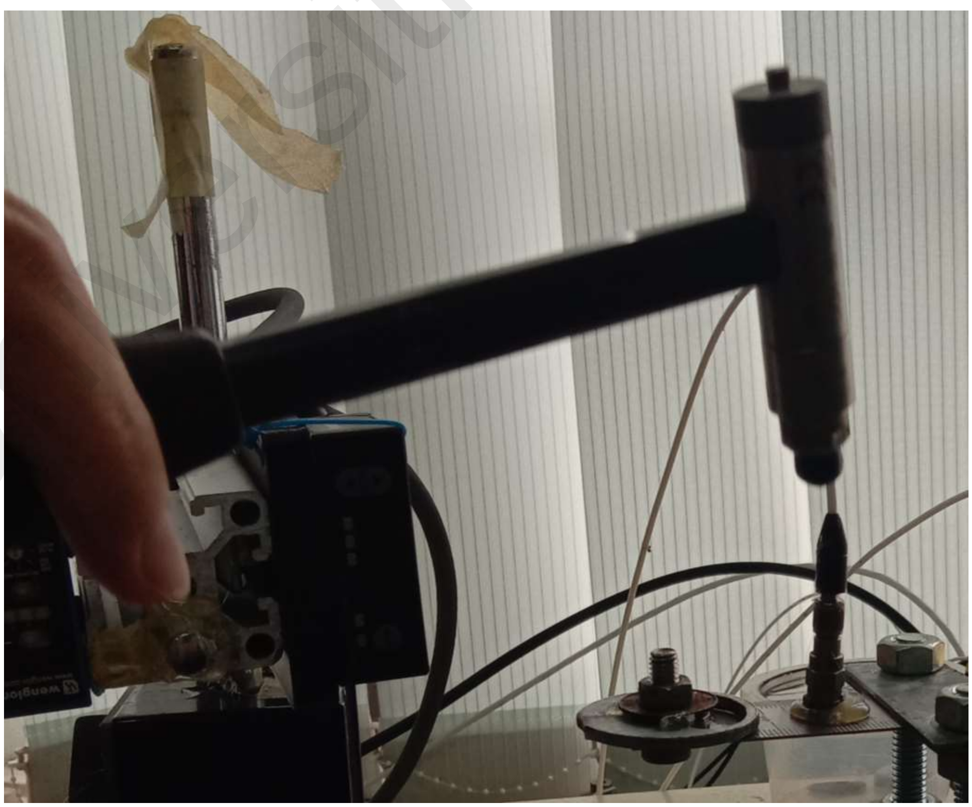

Figure 3-20: Hammer delivering an Impulse to the System

The experiment is conducted 3 times at each disc position. The disc position is locked via glue at 0 degrees, 90 degrees and 180 degrees respectively, with the natural frequency at each position recorded. The natural frequency at first mode is recorded.

Next step is to excite the cantilever-disc system with external vibration via the TiraVib Shaker. The excitation frequency of the shaker is swept from 38Hz to 55Hz in 1 Hz increment for the disc in 0˚, 90˚ and 180˚ position. The input excitation measured by Sensor #2 is set at 2G-RMS and Sensor #1 records the response of the system to the shaker's vibration at various frequencies. The experiment is repeated 3 times for repeatability purposes.

3.5.2 Self-Tuning Behavior of the System

The main objective of this section is to investigate the self-tuning behavior of the system with respect to the external excitation frequency. This is conducted by unlocking the disc so it is free to rotate, and vibrating the system using the TiraVib™ shaker at 2G-RMS as measured by Sensor #2. The vibration frequency is again swept from 39Hz to 55Hz at 1Hz interval, and the position when the disc stops turning is recorded at each excitation frequency. This is again repeated 3 times for repeatability purpose.

3.5.3 Bandwidth of the System

The response of the system to the input forced excitation at 2G-RMS is measured with the disc at the position that it settles at each frequency as obtained in Section 3.5.2. For example, at an excitation frequency of 45Hz, the disc settles at 70˚ position. At 70˚ position, the response of the system as measured by IEPE sensor #1 with an input excitation frequency of 45Hz at 2G-RMS is recorded. This test is continued from 39Hz to 55Hz in 1 Hz increment.

3.5.4 Real Time Amplitude – Self-Tuning

Finally, a real time experiment is conducted where the disc is allowed to rotate, and the beam's displacement amplitude is recorded in real time via a Laser Displacement Sensor. A laser displacement sensor is setup to measure the displacement at the tip of bolt holding the cantilever beam. The laser displacement sensor shines a laser beam to the point of measurement that can be seen. This setup is shown in Figure 3-21. Note the red laser "dot" that can be observed at the tip of the bolt holding the rotating disc.

Figure 3-21: Laser Displacement Sensor Measuring Displacement at Tip of Bolt

The disc is then intentionally placed at a rotary position such that the natural frequency is away from the excitation frequency initially. This is tested twice at with a shaker excitation of 39Hz and 48Hz at 2G-RMS.

i) With the disc placed at 180˚ position initially, the shaker is excited at 39Hz

ii) With the disc placed at 0˚ position initially, the shaker is excited at 48Hz.

This allows the change in vibration amplitude as the system adjusts itself to be observed in real time in both directions. This result is presented in Section 4.4.4.

CHAPTER 4: RESULTS AND DISCUSSION

4.1 Introduction.

This section reports on the results and discussions on the methodologies listed in Chapter 3, organized according to the order of that chapter. Section 4.2 covers the results and discussions for Design, Section 4.3 covers Fabrication and Section 4.4 covers results and discussions from the Experiments conducted to test the fabricated Vibration Harvester.

4.2 Self-Tuning Vibration Harvester Design

As discussed in Section 3.3, the Vibration Harvester is designed based on the following observations

i) Vibration is known to cause loosely supported shaft/disc to rotate.

ii) The rotary position of an asymmetrical disc affects the mass distribution caused by the disc. If this asymmetrical disc is placed at the end of a cantilever beam, the mass distribution of the disc on the beam is a function of the rotary position of the disc. This in turns alters the natural frequency of the mass-cantilever system.

Combining the 2 above, this resulted in the final design is as per Figure 3.1.

During the initial stage, a brake was thought to be needed to lock the asymmetrical disc in position once near resonance is reached to stop the disc from continuing to rotate, which could cause the beam to cycle between resonant state and off resonant state continuously as the disc rotates. However during the initial test, it was observed that the disc, when it is asymmetrical, stops by itself at locations that depends on the frequency of excitation. A possible reason for this behavior is discussed in Section 4.4.2. This then becomes the main focus of subsequent experiments, to determine if this self-stopping behavior can increase the bandwidth of the system.

Another point worth discussing is the on size of the disc and length of the cantilever. During pre-test, 2 disc sizes at 35mm diameter and 50mm diameter were tested. It was found that the 50mm disc were too heavy to be rotated reliably within the power constraint of the TiraVib shaker and amplifier. The current limiter of the Tiravib amplifier were frequency tripped at vibrations levels that rotate the 50mm disc. Hence, the 35mm disc was used in the final design. It was also found that that disc rotates reliably from 39-55Hz. With that, a 55mm cantilever places the natural frequency of the testing apparatus with 35mm disc within this range.

4.3 Fabrication

The parts of the testing apparatus was fabricated as per the methodology in Section 3.4. Once fabricated, the entire system was assembled, and placed on top of a TiraVib shaker using a jig that is already found in the University's Vibration Lab.

The dimensions and other details for the system are described in Table 1

Table 1: Specifications of the Self-Tuning Mass-Cantilever System

Description	
Thickness of Beam	0.64 mm
Width Of Beam	26.10 mm
Length of Supported Beam	55.00 mm
Distance from Beam Support to Center of Rotation Axis	46.00 mm

Diameter of Disc	35.70 mm
Thickness of Disc	2.95 mm
Weight of Disc	12 g
Weight of Bolt/Nut	9 g

The fabrication process was relatively straightforward. Once assembled, prior to starting the experiments, 1x IEPE sensor is placed close to the base of the cantilever as shown in Figure 3-16

The mass of the IEPE accelerometer is approximately 3 grams, which is 25% the mass of the asymmetrical disc. Therefore, the presence of this accelerometer will alter the natural frequency of the setup. This is the reason why the IEPE accelerometer #1 is placed near to the base of the cantilever, to minimize the effect of the sensor's mass to the natural frequency of the self-tuning system.

Another IEPE sensor is required to measure the magnitude of the external vibration that is applied by the TiraVib™ shaker. This would then allow the input vibration magnitude to be set to a constant, or in another word to become an independent variable. This allows IEPE Sensor #1 to measure the response of the beam as a function of excitation frequency only. This Sensor #2 is placed near the base of the jig as shown in Figure 3-18

4.4 Experimental Results

This section covers the results and discussions of all the experiments conducted to test the self-tuning behavior of the Vibration Harvester listed from Section 3.5.1 to Section 3.5.4

4.4.1 Natural Frequency of the System

This section reports on the results from EMA and frequency sweep conducted on the Vibration Harvester as per Section 3.5.1. With the rotating mass locked in 3 different positions, namely at 0˚, 90˚ & 180˚ respectively, the natural frequencies from EMA analysis done in Section 3.5.1 at each position is presented in Figure 4-1.

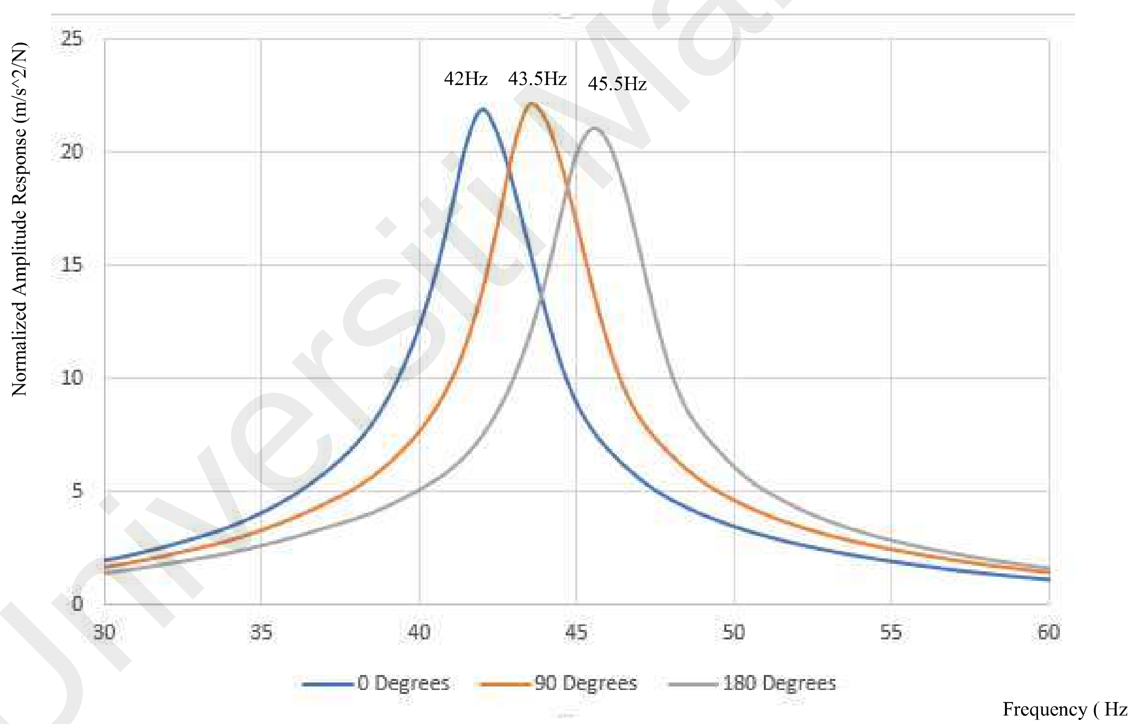

Figure 4-1: Normalized Amplitude Response vs Frequency from EMA Analysis with the Rotating Mass Locked in 3 Positions

From the EMA results, we now know the natural frequencies at the 3 positions are 42Hz, 43.5Hz and 45.5Hz respectively. However, this is only 1 part of the solution. The position of the disc vs excitation frequency will determine if the self-tuning behavior contributes to improved bandwidth of the testing apparatus.

Table 2 : Position of Rotating Disc VS Natural Frequency

	Position	Natural Frequency
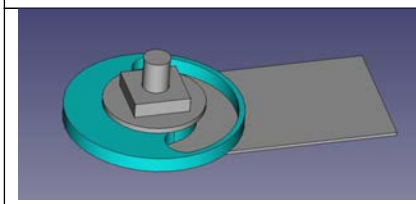	0˚	42 Hz
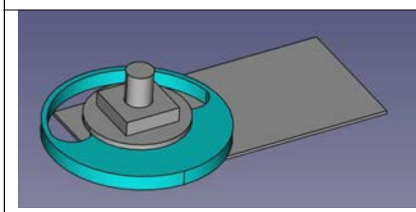	90˚	43.5 Hz
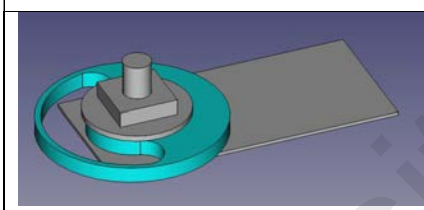	180˚	45.5 Hz

A frequency sweep was also done to verify the results of EMA. As per Section 3.5.1, the testing apparatus at 3 different disc positions is excited by the TiraVib™ shaker from 39Hz to 55Hz with an acceleration of 2G-RMS as measured by IEPE Sensor #2. This test was done 3 times to ensure repeatability and the acceleration measured by IEPE Sensor #1 is plotted in Figure 4-2 to Figure 4-7.

Figure 4-2 to Figure 4-4 shows the frequency sweep of 3 separate tests at different positions overlaid on top of another, and shows that the results are repeatable with minimal variations across the frequency range.

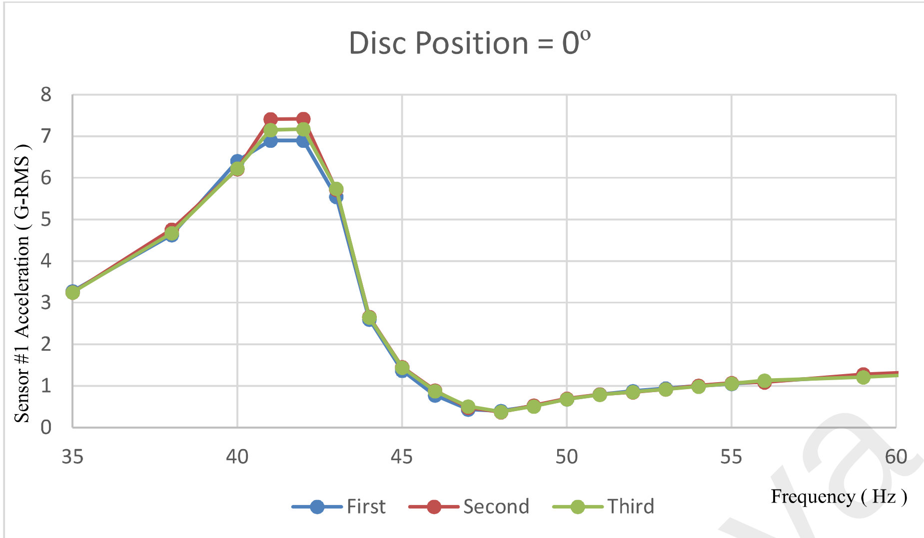

Figure 4-2: Amplitude Response at 0˚. Repeated 3 Times

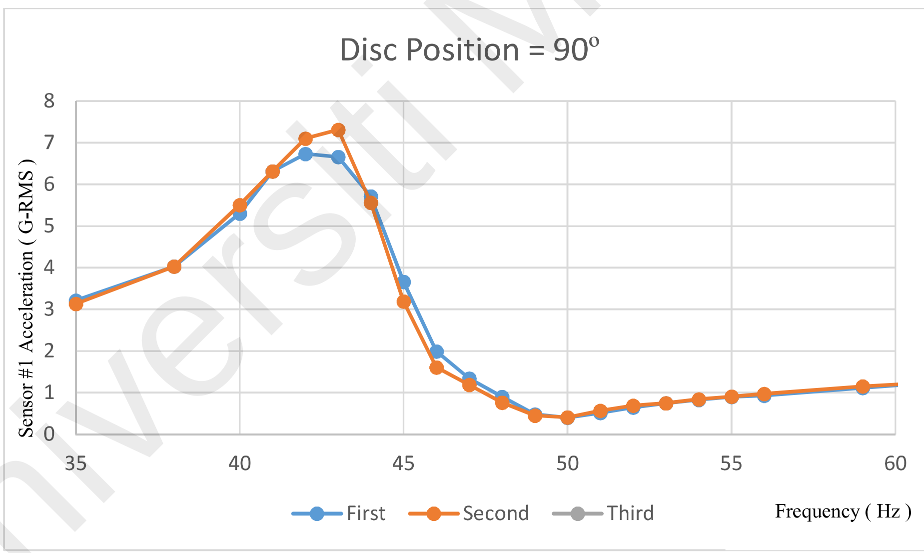

Figure 4-3: Amplitude Response at 90˚. Repeated 3 Times

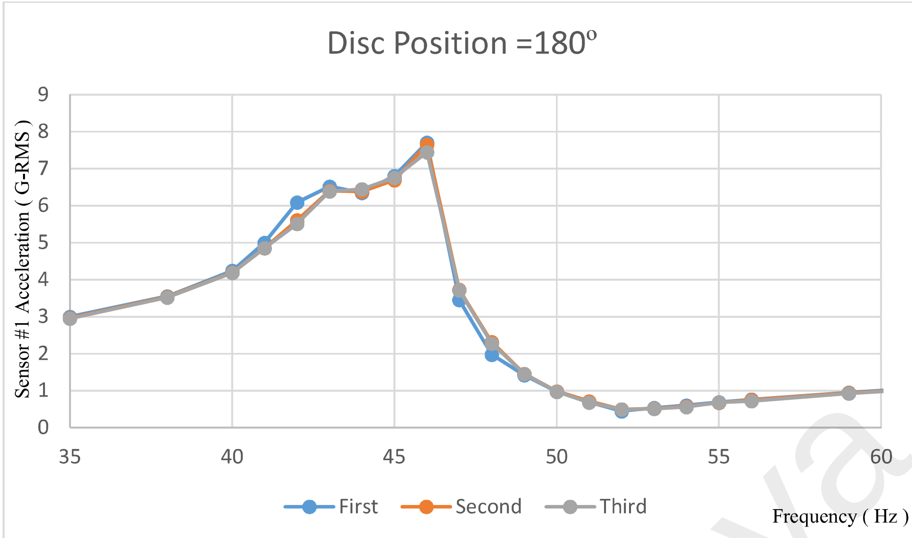

Figure 4-4: Amplitude Response at 180˚. Repeated 3 Times

Putting all 3 curves together for different disc positions yields the results shown in Figure 4-5 to Figure 4-7. This way, the natural frequencies at 3 different positions agree with the results from EMA presented in Table 2, with natural frequency at 0˚ position at 42Hz, at 90˚ position at 43.5 Hz, and 46 Hz at 180˚ position. This proves that, the rotary position affects the mass distribution on the cantilever which in turns, changes the natural frequency of the testing apparatus.

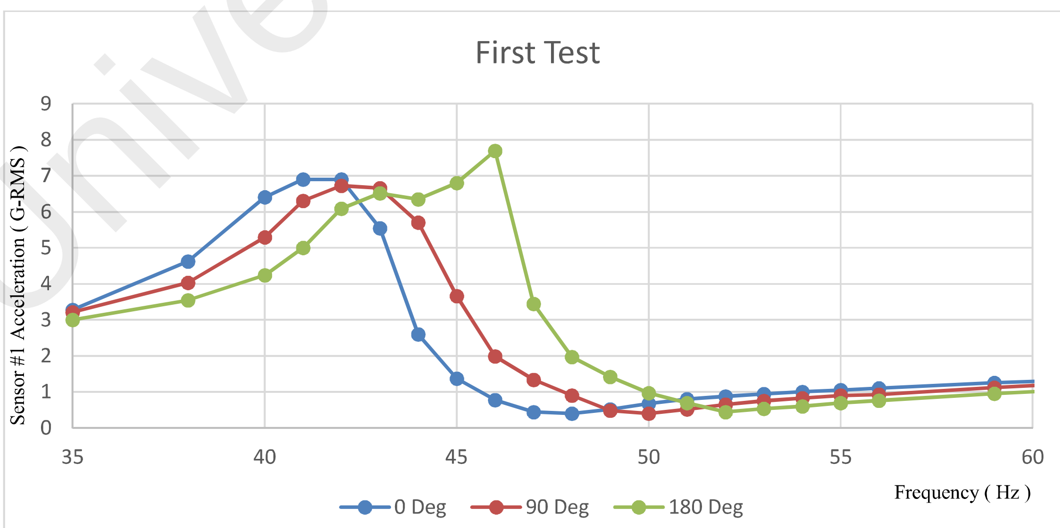

Figure 4-5: Amplitude Response for all 3 Positions. First Trial

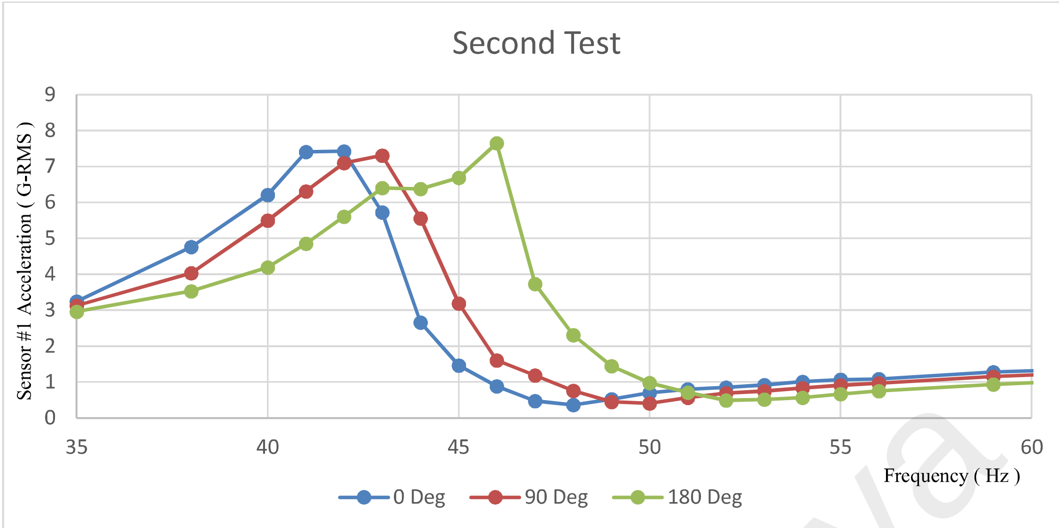

Figure 4-6: Amplitude Response for all 3 Positions. Second Trial

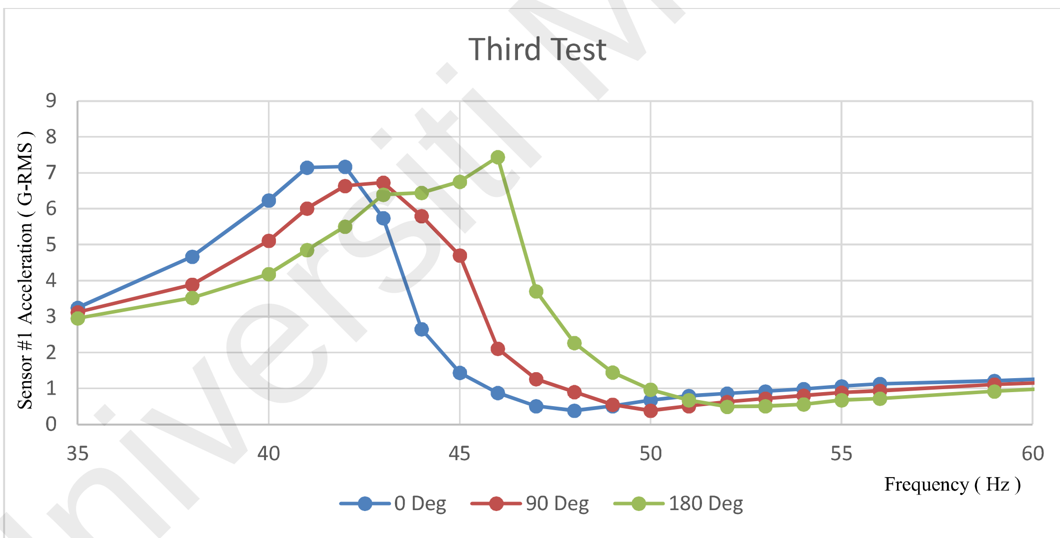

Figure 4-7: Amplitude Response for all 3 Positions. Third Trial

4.4.2 Self-Tuning Behavior of the System

This section reports on the results and discussion obtained from the experiment listed in Section 3.5.2. The settled disc position is observed to vary based on the excitation frequency. The position stays at relatively close to 0˚ up to an excitation of 43Hz. It rises rapidly from 44Hz onwards to about 51Hz, at which above that, the disc settles at 180º position. This experiment was also conducted 3 times to ensure repeatability. Slight variation is observed and the result is plotted in Figure 4-8. However, there is virtually no difference in settled position whether the frequency is swept up (39 –> 55Hz) or swept down (55->39Hz).

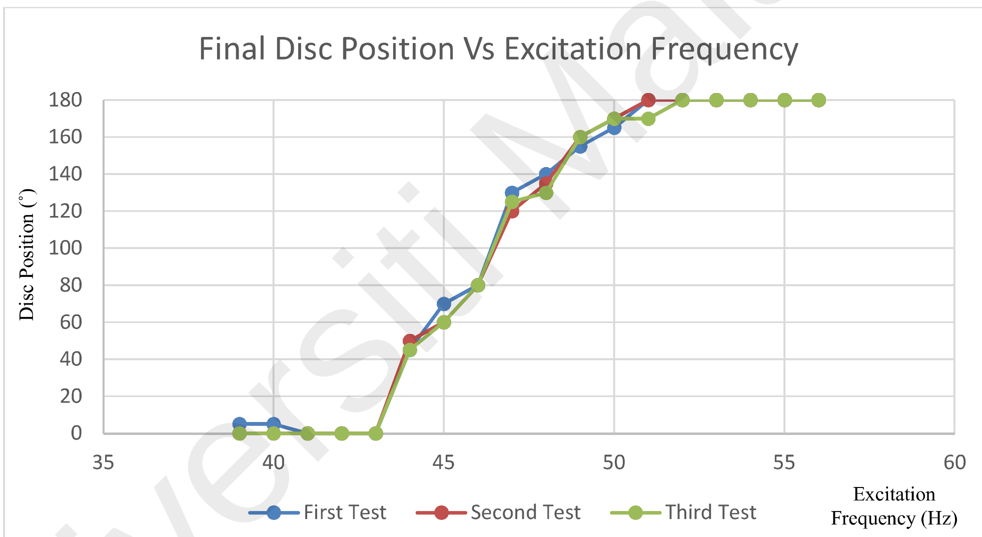

Figure 4-8: Disc Final Settled Position vs Excitation Frequency.

This is an interesting observation, as based on the observation reported in Section 4.4.1, the natural frequency of the Vibration Harvester increases when the position of the disc increases. The result of this section means the natural frequency of the Vibration Harvester increases with increasing excitation frequency.

In this section, we attempt to provide a possible reason why the disc is behaving as per Figure 4-8 that brings forth the self-tuning behavior of the testing apparatus. There are 2 effects at play, namely

i) Centrifugal force on the disc.

At low vibrational amplitudes, most derivation of defining equations for natural frequencies for pendulum or mass-cantilever supported at one end assume that the vibrating particle moves in a straight line (Hibbeler, 2016). At high amplitudes, this assumption is not correct and the particle moves in an arc. As an arc is not a straight line, according to Newton's 1st Law, a net force needs to act on the particle to cause it to move in that arc. This "centrifugal" force or apparent force "felt" by a particle moving in a circle is what pushes the mass on the heavier side of the asymmetrical disc outwards towards the 0˚ position at high amplitudes. In another words, the mass is flung out to 0˚ position. This is the furthest the mass could be flung out. This "flung out" effect at high amplitude is also observed in Lan et al. (2021) setup when excited at the first mode of vibration, which gives credence to this explanation.

ii) At lower amplitudes, when "centrifugal" forces are less dominant, it is observed that the heavier side of the asymmetrical disc tends to settle closer to the beam's support (180˚ position). At first mode of vibration, points closer to the support has lower displacement compared to the point closer to the tip of the cantilever. This "settling on nodes" is analogous to what is observed in high school physics experiment where an acoustic standing wave is set up in a tube lined with dust/powder at the bottom of the tube initially. The standing waves formed will push the dust at the bottom towards the node, or the point with lower to no vibration. The same effect is also observed with sand on a plate. Vibration of the plate causes the sand to settle on nodes, creating patterns called Chladni Figures (Rzepecki et al., 2020). Since the disc is free to rotate, this effect is believed to be what driving the disc towards the 180˚ position at low amplitudes. This settling of mass towards the beam's support at high frequencies is also noted by Bukhari et al. (2020) in their self-tuning vibration harvesting system.

Therefore, the 'tug-of-war' between the 2 effects above is believed to be causing the disc to behave as per Figure 4-8. At lower amplitudes, the disc tends to move towards 180˚ position due to settling on nodes, and at higher amplitudes, the disc tends to move towards the 0˚ due to centrifugal forces.

If we compare this result to the result obtained by Shin et al. (2020), Shin's setup was able to lock at resonant position, while the setup in this study was not able to lock at resonant position. To illustrate this point, the natural frequency at 90˚ position is 43.5Hz, but it takes an excitation frequency of 46Hz before the disc is able to settle near 90˚ position. The same applies to the 180˚ position where the natural frequency at 180˚ position is 45.5Hz, but it takes an excitation of 51Hz before the disc can settle on the 180 degree position. In short, the increase in natural frequency of the setup in this study lags the increase in excitation frequency. Thus there is lagging effect, unlike the setup in Shin et al. (2020) where their setup is able to lock at resonant position.

A possible reason is provided. Let's consider what happens to the disc at 90 degree position, when excited with an external excitation of 43.5Hz. At those positions and excitation frequency, resonance will happen and large amplitudes will be expected. However, large amplitudes causes the mass to be flung away from those positions due to centrifugal forces. Shin et al. (2020) setup is locked at both ends as per

Figure 4-10 , and thus not affected by centrifugal forces even at high amplitudes while in this study, the cantilever beam is only locked at one end (Figure 4-9)

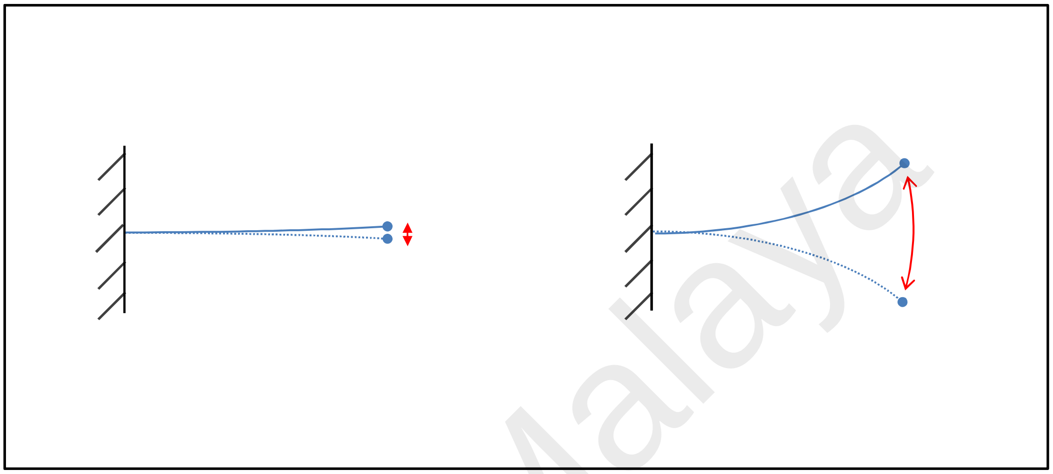

Figure 4-9: Cantilever Locked at One End, At High Amplitudes, the Mass at the Tip Moves in an Arc

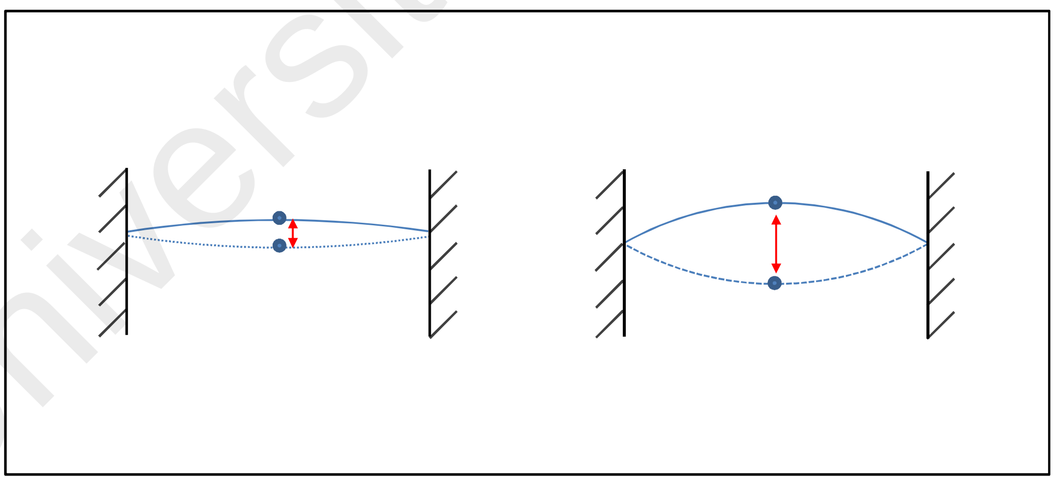

Figure 4-10: Cantilever Locked at Both Ends. At High Amplitudes, the Mass Moves in a Straight Line.

4.4.3 Bandwidth of the System

This section reports on the result and discussion obtained from the experiment in Section 3.5.3. With the disc settled down in the position shown in Figure 4-8, the frequency response of the testing apparatus is shown in Figure 4-11, overlaid on top of the response of the testing apparatus with the disc locked at 0 º position.

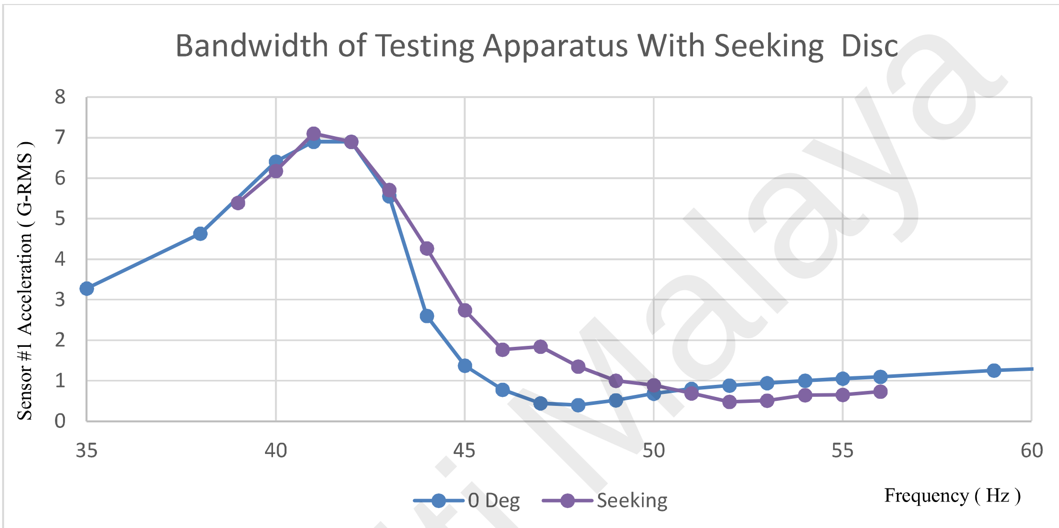

Figure 4-11: Bandwidth of Testing Apparatus compared to Bandwidth at 0° Position

Table 3: Acceleration Values of Disc Locked at 0° vs Self Tuning.

Frequency (Hz)	Acceleration at Sensor #1 with Disc at 0º (G-RMS)	Acceleration at Sensor #1 with Disc allowed to Turn (G-RMS)	% Difference
40	6.41	6.18	-3.6 %
41	6.90	7.10	+2.9 %
42	6.90	6.90	0 %
43	5.55	5.71	+2.8 %
44	2.60	4.27	64.2 %
45	1.37	2.74	100.0 %
46	0.78	1.77	126.9 %

47	0.44	1.84	318.2 %
48	0.40	1.35	237.5 %
49	0.52	1.00	92.3 %
50	0.68	0.89	30.9 %
51	0.80	0.69	- 13.5%
52	0.88	0.48	-45.5 %
53	0.94	0.51	- 45.7 %
54	1.00	0.64	- 36 %
55	1.05	0.65	- 38 %

It is clear from Table 3 and Figure 4-11, that with the disc released and allowed to self-tune, the bandwidth is larger compared to with the disc locked at 0˚. At 47Hz, the self-tuning property of the disc causes the Vibration Harvester to vibrate at a G-RMS that is 318.2% higher compared to when it is locked at 0˚ position for the same external excitation. This larger vibration amplitude is expected to generate a larger amount of electrical energy in vibration harvesting applications regardless of the harvesting method used (piezo element or magnet-coil system).

As discussed in Section 4.4.2, the implication of the result in Figure 4-8 is the natural frequency of the Vibration Harvester increases with increasing excitation frequency. Hibbeler (2016) shows that the amplitude of forced excitation depends on the difference between excitation frequency and natural frequency. The smaller the difference, the higher the amplitude of forced vibration.

The increase in natural frequency of the Vibration Harvester as the excitation frequency is increased causes the difference between excitation and natural frequency to be lower compared to if the disc is locked at 0˚. This reduced difference between excitation frequency and natural frequency increases the amplitude of forced excitation compared to when the disc is locked and not allowed to seek.

Also discussed in Section 4.4.2, the setup in this study is unable to lock at resonant position at 43.5Hz to 45.5Hz. The increase in natural frequency of the system “lags” the increase in excitation frequency. Therefore, we could not obtain a flat frequency response like the ones obtained by Shin et al. (2020).

The size of the Bandwidth depends on how the cut off in frequency and amplitude are defined. In this study, the disc rotates reliably from 39Hz to 55Hz. Thus, if we focus primarily on 39-55Hz and define the cut off as 50% of maximum amplitude, the improvement in bandwidth of the self seeking system (BW 2) compared to the non self seeking system (BW 1) can be approximated as 0.9 Hz as shown in Figure 4-12.

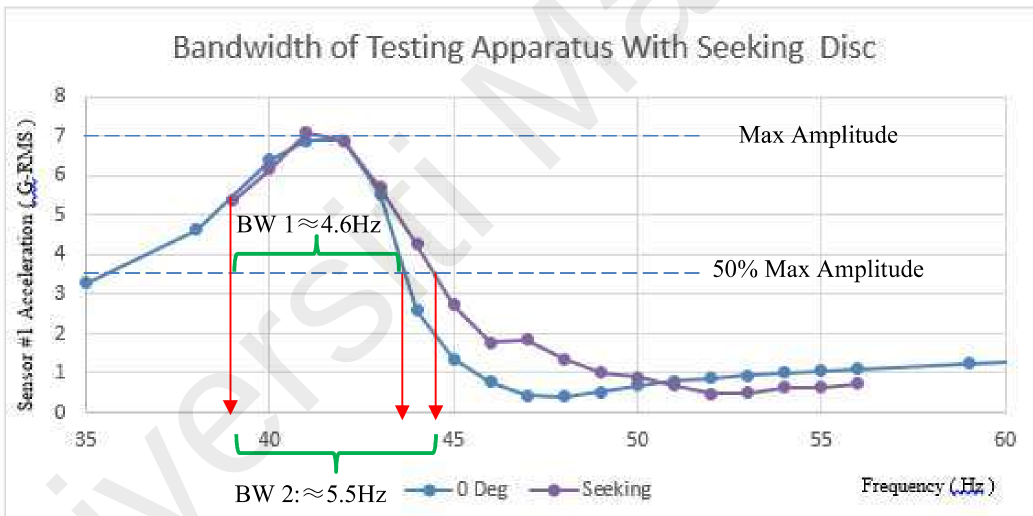

Figure 4-12: Definition and Improvement in Vibration Amplitude Bandwidth

4.4.4 Real Time Amplitude - Self Tuning

This section reports on the results and discussion obtained from the experiment in Section 3.5.4. A laser displacement sensor was used to measure the actual displacement amplitude at the tip of the bolt holding the rotating disc and it is measured vs time. This setup can be seen in Figure 3-21. With the Disc placed at an initial position of 180˚ and with the external excitation at 39Hz, the amplitude response in real time is shown in Figure 4-13.

At 180˚ position, the natural frequency is 45.5Hz. Self-tuning behavior is observed in Figure 4-13 when the amplitude increases as the disc rotates to the final settled position at 0˚. This is an indication that the system can self-tune with decreasing excitation frequency. It is able to adjust the natural frequency from 45.5Hz to 42Hz, in response to a low excitation frequency.

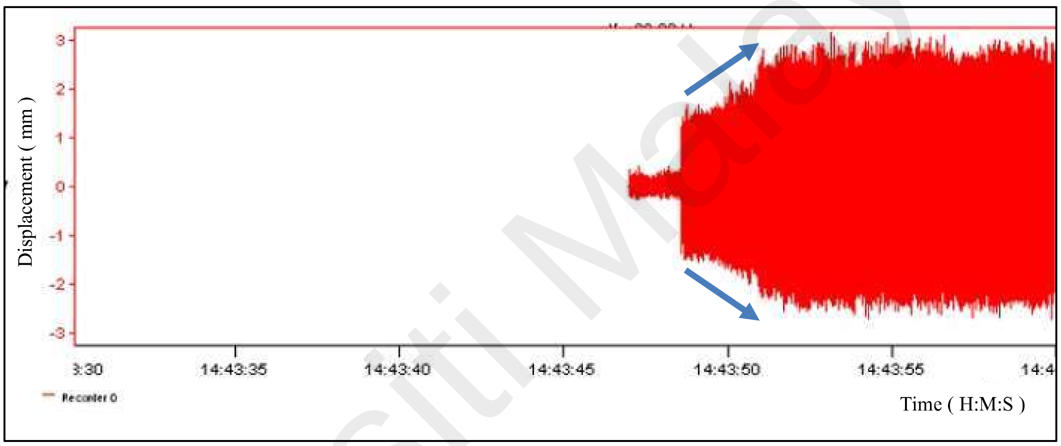

Figure 4-13: Real Time Amplitude at 39Hz. Disc Initial Position = 180˚

The same self-tuning behavior is also observed in Figure 4-14 when the excitation frequency is at 49Hz. The disc initial position is placed at 0˚. At 0˚, the natural frequency is 42Hz. As the disc rotates to the final settled position at 160˚ as indicated in Figure 4-8 for 49Hz, the amplitude increases. This is an indication that the system can self-tune with increasing excitation frequency. It is able to adjust the natural frequency from 42Hz to about 45.5Hz in response to a higher excitation frequency.

Thus, the Vibration Harvester designed and fabricated in this study is able to adjust its natural frequency in both directions.

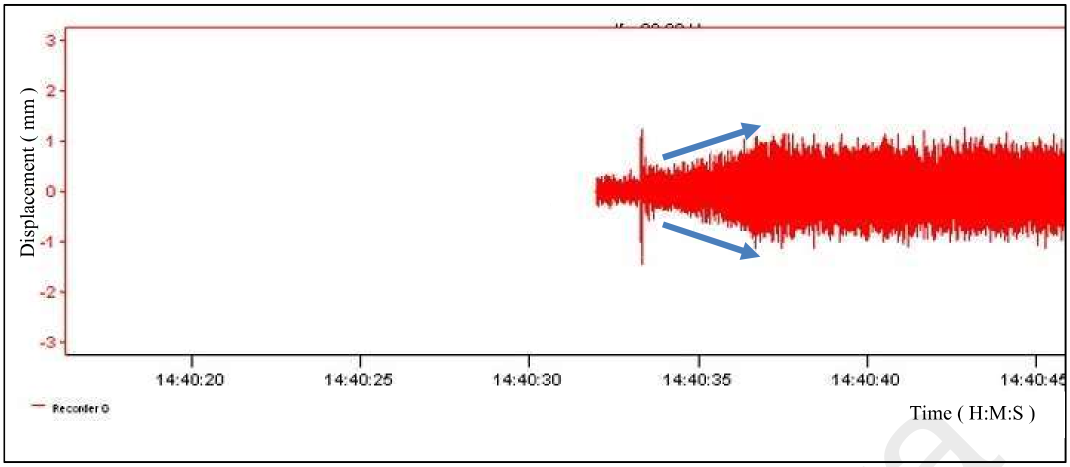

Figure 4-14: Real Time Amplitude at 49Hz. Disc Initial Position = 0˚

CHAPTER 5: CONCLUSION AND RECOMMENDATIONS

5.1 Conclusion

Self Tuning Vibration Harvester is successfully designed combining the observation that vibration turns a loosely supported disc and an asymmetrical disc attached to the end of a cantilever causes the natural frequency of the cantilever to be a function of rotary position of the disc.

The Vibration Harvester is fabricated using 35mm steel washer with a portion of the steel removed to make it asymmetrical. The disc is placed at the end of a cantilever beam and is free to rotate. The maximum axial displacement or gap that the disc can move relative to the cantilever is 0.7mm. This gap was selected because reliable disc rotation was observed during tests. Gaps that are too small cause the rotation to be erratic.

Several experiments were conducted to test the self-tuning properties of the fabricated Vibration Harvester. It is concluded from the experiments that an asymmetrical disc that is free to rotate on a cantilever beam has self-tuning properties that can be used to increase the bandwidth of a Vibration Harvesting System. At an excitation frequency of 47Hz, the self-tuning behavior allows the cantilever beam to vibrate with an acceleration magnitude that is 318% higher than the vibration of the cantilever beam without the self-tuning behavior. This increase in vibration contributed by the self-tuning behavior is noted until an excitation frequency of 50 Hz. It is also verified experimentally that the self-tuning behavior works both ways with increasing and decreasing excitation frequencies. Finally, an increase in Bandwidth of $\approx$ 0.9Hz is observed. The increase in bandwidth is limited by the effects of centrifugal force that causes the increase in natural frequency of the system to lag the increase in excitation frequency applied to the system.

5.2 Recommendations

- In this research, it was observed that the gap that the asymmetrical disc is allowed to move has a large effect on the self-tuning behavior of the disc. It is recommended that a complete study on the effects of gap on the self –tuning behavior of the system is conducted.

- It is found from this research that the observed self-tuning behavior does not "lock" the disc at 90˚ and 180˚ position when the excitation frequencies are at the natural frequencies of those positions due to "centrifugal" forces flinging the asymmetrical disc away from those positions. There are mechanisms that passively convert axial vibration motion into rotary motion available such as those proposed by Altshuler, Pastor, Garcimartín, Zuriguel, and Maza (2013). With additional torque generated by such devices, it could potentially counter the centrifugal forces and keep the disc closer to 90˚ and 180˚ positions when the excitation frequencies are at the natural frequencies of those positions. This would potentially result in a flatter frequency response and a larger bandwidth.

Figure 5-1: A Passive Device that Converts Vibration Motion into Rotary Motion. (Altshuler et al., 2013)

- The size/mass of the disc affect the natural frequency range of the cantilever as the disc rotates from 0˚ to 180˚. A study on the effects of size or mass ratio of the disc to the bandwidth and self tuning behavior need to be conducted to increase the bandwidth of the self tuning system.

- In this research, only the physical aspects of the vibration is studied. It is expected that larger vibrational amplitude will cause larger amount of electrical energy to be generated. If a piezo element or magnet-coil system is added, energy is being removed from the system, which can be thought of as damping. It is recommended that a study is conducted on the effects that the addition of such system to the self-tuning behavior of the system.

- As the disc rattles in the axial gap, significant noise is observed. This needs to be improved in future iterations of the self tuning mechanism.

REFERENCES

Altshuler, E., Pastor, J. M., Garcimartín, A., Zuriguel, I., & Maza, D. (2013). Vibrot, a Simple Device for the Conversion of Vibration into Rotation Mediated by Friction: Preliminary Evaluation. *PLOS ONE, 8*(8), e67838. doi:10.1371/journal.pone.0067838

Bukhari, M., Malla, A., Kim, H., Barry, O., & Zuo, L. (2020). On a self-tuning sliding-mass electromagnetic energy harvester. *AIP Advances, 10*(9), 095227. doi:10.1063/5.0005430

Chen, D. M., Dai, X. N., & Tang, Z. B. (2020). Estimate method research at working life of wireless sensor network nodes. *Journal of Physics: Conference Series, 1678*, 012095. doi:10.1088/1742-6596/1678/1/012095

Cundeva-Blajer, M., & Srbinovska, M. (2018). Mathematical Tools for Optimization of Energy Consumption in Wireless Sensor Networks. *Journal of Physics: Conference Series, 1065*, 212013. doi:10.1088/1742-6596/1065/21/212013

Fu, H., Sharif-Khodaei, Z., & Aliabadi, M. H. F. (2019). An energy-efficient cyber-physical system for wireless on-board aircraft structural health monitoring. *Mechanical Systems and Signal Processing, 128*, 352-368. doi:https://doi.org/10.1016/j.ymssp.2019.03.050

Hibbeler, R. (2016). Engineering Mechanics, Dynamics. 14th Edition.

IEA. (2020). Renewables, 2020. Retrieved from https://www.iea.org/reports/renewables-2020

Khan, F. U., & Iqbal, M. (2018). Electromagnetic Bridge Energy Harvester Utilizing Bridge's Vibrations and Ambient Wind for Wireless Sensor Node Application. *Journal of Sensors, 2018*, 3849683. doi:10.1155/2018/3849683

Lallart, M., Anton, S. R., & Inman, D. J. (2010). Frequency Self-tuning Scheme for Broadband Vibration Energy Harvesting. *Journal of Intelligent Material Systems and Structures, 21*(9), 897-906. doi:10.1177/1045389X10369716

Lan, C., Chen, Z., Hu, G., Liao, Y., & Qin, W. (2021). Achieve frequency-self-tracking energy harvesting using a passively adaptive cantilever beam. *Mechanical Systems and Signal Processing, 156*, 107672. doi:https://doi.org/10.1016/j.ymssp.2021.107672

Li, D., Han, J., Li, L., & Wang, W. (2017, 27-30 Oct. 2017). *Effect of the centroid position of cantilever beam on the performance of PVDF energy harvester device.* Paper presented at the 2017 Symposium on Piezoelectricity, Acoustic Waves, and Device Applications (SPAWDA).

Li, X., Yu, K., Upadrashta, D., & Yang, Y. (2019). Comparative study of core materials and multi-degree-of-freedom sandwich piezoelectric energy harvester with inner cantilevered beams. *Journal of Physics D: Applied Physics, 52*(23), 235501. doi:10.1088/1361-6463/ab0aae

Melchor-Martínez, E. M., Macias-Garbett, R., Malacara-Becerra, A., Iqbal, H. M. N., Sosa-Hernández, J. E., & Parra-Saldívar, R. (2021). Environmental impact of emerging contaminants from battery waste: A mini review. *Case Studies in Chemical and Environmental Engineering, 3*, 100104. doi:https://doi.org/10.1016/j.cscee.2021.100104

Park, H., Lee, D., Park, G., Park, S., Khan, S., Kim, J., & Kim, W. (2019). Energy harvesting using thermoelectricity for IoT (Internet of Things) and E-skin sensors. *Journal of Physics: Energy, 1*(4), 042001. doi:10.1088/2515-7655/ab2f1e

Perez, M., Chesné, S., Jean-Mistral, C., Billon, K., Augez, R., & Clerc, C. (2020). A two degree-of-freedom linear vibration energy harvester for tram applications. *Mechanical Systems and Signal Processing, 140*, 106657. doi:https://doi.org/10.1016/j.ymssp.2020.106657

Rzepecki, J., Chraponska, A., Budzan, S., Isaac, C. W., Mazur, K., & Pawelczyk, M. (2020). Chladni Figures in Modal Analysis of a Double-Panel Structure. *Sensors, 20*(15). doi:10.3390/s20154084

Sachan, S., Sharma, R., & Sehgal, A. (2021). Energy efficient scheme for better connectivity in sustainable mobile wireless sensor networks. *Sustainable Computing: Informatics and Systems, 30*, 100504. doi:https://doi.org/10.1016/j.suscom.2020.100504

Shahruz, S. M. (2006). Design of mechanical band-pass filters with large frequency bands for energy scavenging. *Mechatronics, 16*(9), 523-531. doi:https://doi.org/10.1016/j.mechatronics.2006.04.003

Shin, Y.-H., Choi, J., Kim, S. J., Kim, S., Maurya, D., Sung, T.-H., . . . Song, H.-C. (2020). Automatic resonance tuning mechanism for ultra-wide bandwidth mechanical energy harvesting. *Nano Energy, 77*, 104986. doi:https://doi.org/10.1016/j.nanoen.2020.104986

Staaf, L. G. H., Köhler, E., Soeiro, M., Lundgren, P., & Enoksson, P. (2015). Smart design selftuning piezoelectric energy harvester intended for gas turbines. *Journal of Physics: Conference Series, 660*, 012125. doi:10.1088/1742-6596/660/1/012125

Sunithamani, S., Rooban, S., Nalinashini, G., & Rajasekhar, K. (2020). A review on mems based vibration energy harvester cantilever geometry (2015–2020). *Materials Today: Proceedings*. doi:https://doi.org/10.1016/j.matpr.2020.11.154

Tang, W. H., Lin, T. K., Chen, C. T., Fu, Y. H., Lin, S. C., & Wu, W. J. (2018). A High Performance Piezoelectric Micro Energy Harvester Based on Stainless Steel Substrates. *Journal of Physics: Conference Series, 1052*, 012038. doi:10.1088/1742-6596/1052/1/012038

Vellucci, F., Sglavo, V., Pede, G., Pasca, E., Malvaldi, V., & Scalari, S. (2014, 29 Oct.-1 Nov. 2014). *Life cycles test on a lithium battery system.* Paper presented at the

IECON 2014 - 40th Annual Conference of the IEEE Industrial Electronics Society.

Waterbury, A. C., & Wright, P. K. (2013). Vibration energy harvesting to power condition monitoring sensors for industrial and manufacturing equipment. *Proceedings of the Institution of Mechanical Engineers, Part C: Journal of Mechanical Engineering Science, 227*(6), 1187-1202. doi:10.1177/0954406212457895

Xue, H., Hu, Y., & Wang, Q. (2008). Broadband piezoelectric energy harvesting devices using multiple bimorphs with different operating frequencies. *IEEE Transactions on Ultrasonics, Ferroelectrics, and Frequency Control, 55*(9), 2104-2108. doi:10.1109/TUFFC.903

Yildirim, T., Ghayesh, M. H., Li, W., & Alici, G. (2017). A review on performance enhancement techniques for ambient vibration energy harvesters. *Renewable and Sustainable Energy Reviews, 71*, 435-449. doi:https://doi.org/10.1016/j.rser.2016.12.073

Zhang, H. T. (2018). Key Technologies of Wireless Sensor Networks: A Review. *Journal of Physics: Conference Series, 1087*, 062014. doi:10.1088/1742-6596/1087/6/062014

Zhu, D., Tudor, M., & Beeby, S. (2010). TOPICAL REVIEW: Strategies for increasing the operating frequency range of vibration energy harvesters: a review. *Measurement Science & Technology - MEAS SCI TECHNOL, 21*. doi:10.1088/0957-0233/21/2/022001